

TECHNISCHE UNIVERSITÄT MÜNCHEN

Institut für Radiologie des Klinikums rechts der Isar München

The Effect of MR Contrast Agents on the Viability and Differentiation Capacity of Human Mesenchymal Stem Cells

Elisabeth Fucini

Vollständiger Abdruck der von der Fakultät für Medizin der Technischen Universität
München zur Erlangung des akademischen Grades eines

Doktors der Medizin

genehmigten Dissertation.

Vorsitzender: Univ.-Prof. Dr. P. Henningsen

Prüfer der Dissertation:

1. Univ.-Prof. Dr. E.J. Rummeny
2. Priv.-Doz. Dr. K. Holzapfel

Die Dissertation wurde am 21.12.2011 bei der Technischen Universität München
eingereicht und durch die Fakultät für Medizin am 08.05.2013 angenommen.

OUTLINE

1.	Introduction.....	4
2.	Background	6
	2.1. Human Mesenchymal Stem Cells and their Clinical Applications.....	6
	2.2. Cell Labeling with MRI Contrast Agents.....	10
	2.2.1. Overview.....	10
	2.2.2. Gadolinium Chelates.....	11
	2.2.3. Iron Oxide Nanoparticles.....	12
	2.2.3.1. Ferumoxides.....	13
	2.2.3.2. Ferucarbotran.....	13
	2.2.4. Cell Labeling Techniques.....	15
	2.3. Differentiation of hMSCs.....	17
	2.3.1. Overview.....	17
	2.3.2. The Chondrogenic Pathway.....	19
3.	Material and Methods.....	25
	3.1. Human Mesenchymal Stem Cells.....	25
	3.2. Labeling of hMSCs.....	26
	3.3. Chondrogenic Differentiation of labeled hMSCs.....	27
	3.4. MR Imaging and Data Analysis.....	27
	3.5. Spectrometry.....	29
	3.6. Histology.....	30
	3.7. Glycosaminoglycan Quantification.....	31

4.	Results.....	32
4.1.	Chondrogenic Differentiation of hMSCs.....	32
4.2.	MR Imaging and Data Analysis.....	34
4.3.	Spectrometry.....	35
4.4.	Histology.....	37
4.4.1.	Safranin O.....	37
4.4.2.	Alcian Blue.....	39
4.5.	Glycosaminoglycan quantification.....	41
5.	Discussion.....	43
6.	Summary.....	46
7.	Bibliography.....	47
8.	Index of Tables and Figures.....	56
9.	Acknowledgement.....	58

1. Introduction

Human mesenchymal stem cells have recently been reported to have a great potential in the repair of a variety of tissues. They have the ability to differentiate into various cell types of mesenchymal origin, ranging from muscle over adipose tissue and bone to articular cartilage (Kostura et al., 2004; El-Badri et al., 2004; Prockop et al., 2003). HMSCs are easily extracted from adult tissues like bone marrow, adipose tissue and skeletal muscle (Barry, Murphy, 2004).

Nowadays, joint replacements are the most effective way to treat cartilage defects caused e.g. by trauma or degenerative processes (Mao, 2005; Lee et al., 2004). Researchers have been focusing on new ways to regenerate cartilage, such as the transplantation of autologous chondrocytes. This method has definitely potential in joint regeneration, however, it cannot fully replace articular cartilage (Brittberg et al., 1994). Out of all ways, the infusion or transplantation of bone-marrow-derived human mesenchymal stem cells is the most promising, as these cells have an extensive capacity for proliferation and great chondrogenic potential when stimulated with specific growth factors, such as TGF- β 3 (Jorgensen et al., 2004; Toh et al., 2005). Problems like immunorejection, as it is found in the implantation of foreign tissues, and the limited life span of prostheses would be overcome by the use of stem cells.

Implanted cells cannot be localized by MRI without the use of contrast agent. For example, superparamagnetic iron oxide (SPIO) nanoparticles have been successfully used to label cells, providing researchers with the possibility to track the biodistribution and migration of these cells by MRI (Bulte et al., 2002; Kostura et al., 2004). It is important to determine whether this kind of labeling affects the viability and differentiation capacity of human mesenchymal stem cells.

Ferumoxides is a US-based, FDA-approved, commercially available superparamagnetic iron oxide, that has been successfully used in previous studies to label human mesenchymal stem cells. Complexing of a transfection agent, like protamine sulfate, to ferumoxides, has turned out to be an effective labeling technique (Arbab et al., 2003; Arbab et al., 2004; Arbab et al., 2005; Kostura et al., 2004).

Ferucarbotran is a Europe-based, especially in liver imaging approved second generation SPIO that can be used to label cells by simple incubation (Hsiao et al., 2007).

In initial studies, no alteration of the viability or differentiation capacity of human mesenchymal stem cells was detected when labeled with ferumoxides and protamine sulfate (Arbab et al., 2004; Arbab et al., 2005). Neither did ferucarbotran-labeling affect the cellular

behavior of stem cells (Hsiao et al., 2007). However, Kostura and colleagues stated an inhibition of chondrogenesis in mesenchymal stem cells labeled with ferumoxides and transfection agent poly-L-lysine (PLL) (Kostura et al., 2004).

The aim of this study was to compare different labeling techniques for human mesenchymal stem cells, that is (1) simple incubation with ferucarbotran, (2) transfection with ferucarbotran and protamine sulfate, and (3) transfection with ferumoxides and protamine sulfate. These techniques were examined with regard to labeling efficiency and changes in viability or chondrogenic differentiation capacity compared to non-labeled controls.

2. Background

2.1. Human Mesenchymal Stem Cells and their Clinical Applications

Stem cells are defined as cells with an unlimited capacity for cell divisions and an undifferentiated phenotype. They have the ability to differentiate to more than one cell lineage. Stem cells can be found in both the developing and the adult organism, and consequently, play roles in organ formation during development and in tissue regeneration. Stem cells are components of normal tissue in various organs, where they have a great capacity for proliferation, as for example mesenchymal stem cells in bone marrow (Fox et al., 2007; Garcia-Castro et al., 2008). In vivo, stem cells function as reservoirs of undifferentiated cells that have the ability to regenerate tissues in case of disease, for example (Barry, Murphy, 2004). Of concern is the potential of some stem cell populations to form teratomas or other tumors (Rapp et al., 2008). Malignant astrocytomas, e.g., have developed from neural stem cells (Alcantara et al., 2009).

Stem cells have been classified according to their abilities to regenerate tissues. There are three kinds of stem cells: Omnipotent stem cells are able to turn into every cell type of the organism. Pluripotent stem cells can give rise to tissues of all three germ layers, but cannot develop into a whole organism. Multipotent stem cells can generate multiple tissue types, but not of all three germ layers (Marshak). For example, the fertilized egg and its progeny from the first few cell divisions is an omnipotent stem cell. Examples for pluripotent stem cells include embryonic stem cells, derived from the inner cell mass of the pre-implantation embryo (Marshak). Sources of multipotent stem cells, such as hematopoietic stem cells and mesenchymal stem cells, are neonatal tissues, like the umbilical cord, and certain adult somatic tissues, including bone marrow, periosteum, trabecular bone, synovium, adipose tissue, skeletal muscle and deciduous teeth (Barry, Murphy, 2004).

The adult bone marrow is the most common source for human mesenchymal stem cells (hMSCs). This can be easily harvested from the superior iliac crest of the pelvis (Digirolamo et al., 1999). HMSCs can act as a precursor for all musculoskeletal and connective tissues found throughout the body, that is bone, cartilage, muscle, tendon, and fat. Therefore, they need to be cultured in certain conditions and treated with particular growth factors (Garcia-Castro et al., 2008). One specific quality of hMSCs is their ability to regenerate injured tissue due to their ease of isolation and the possibility of a rapid amplification (Jorgensen et al., 2004).

This offers new opportunities for the treatment of pathologies in mesenchymal tissues, ranging from cardiac muscle to bone and joint regeneration (Csaki et al., 2008). Additionally, hMSCs could be used for the treatment of autoimmune diseases, as they modulate immune

function and contribute to hematopoiesis. Clinical trials on these therapies are being carried out (Garcia-Castro et al., 2008; El-Badri et al., 2004).

Researchers have been focusing on new ways of improving the repair of bone and cartilage, as reconstructive surgery is currently the most effective way to treat the loss of cartilage substance after trauma or at advanced stages of rheumatoid arthritis. Total joint replacement is the most common practice to treat osteochondral lesions, but it has major disadvantages like possible pathogen transmission and a limited life span of the implant. Consequently, clinicians and scientists have been trying to regenerate synovial joint components that integrate into the joint and remain functional for a life time (Mao, 2005).

Therefore, efforts have been made to implant bone marrow, bone marrow scaffold composites, and chondrocytes into cartilage defects (Lee et al., 2004; Giannoni et al., 2005). In a recent study, bone marrow aspirate in combination with hyaluronic acid was directly implanted into articular cartilage defects of goats, resulting in good cartilage repair (Saw et al., 2009). Chondrocyte transplantation is a promising new concept of cell therapy with the possibility to regenerate cartilage, even though problems like an uneven distribution of the transplanted cells, the leakage of grafted chondrocytes, and differentiation into undesired fibrocartilage have arisen. Recently, an even more promising cell source has been discovered: hMSCs, which are thought to have a higher chondrogenic potential *in vitro* (Jorgensen et al., 2004; Lee et al., 2004). Before hMSCs can replace autologous chondrocytes in the treatment of articular cartilage defects, much more preclinical and clinical trials are necessary (Csaki et al., 2008).

In a first study, hMSCs were implanted into the arthritic joints of New Zealand white rabbits, where they differentiated into chondrocytes that secreted a cartilaginous matrix (Wakitani et al., 1994). However, the repaired tissue lost stability over time by thinning and a discontinuity between the host tissue and the new tissue was detected. Subsequent experimental studies showed that MSCs injected in knee joints were able to regenerate cartilage if stimulated with growth factors, e.g. BMP-2 (bone morphogenetic protein) or IGF-1 (insulin-like growth factor) (Gelse et al., 2003).

Applications of cell therapies in patients are still limited due to problems with large-scale expansion of cells in general and associated high costs. hMSCs might overcome these problems, since they have an extensive capacity for proliferation and can differentiate into multiple cell types (Fox et al., 2007). There are difficulties in the clinical application of hMSCs though, because selective growth factors and scaffolds that keep the cells in the differentiated state have to be tested and used *in vivo* (Jorgensen et al., 2004). Besides, after two to three months of culturing, proliferation rate and differentiation capacity of MSCs has shown to decrease due to senescence (Wagner et al., 2010). This process is not quite understood yet, but possible explanations are mutations and cellular defects that accumulate in

cells during long-term culture. Self-renewal and cell division might also be restricted under these conditions (Wagner et al., 2010).

In conclusion, stem cells are at the frontier in regenerative medicine, including cell therapy, gene therapy, and tissue engineering. However, more preclinical studies have to take place before hMSCs can be used for clinical therapy, because their long-term behavior is still unknown.

The synovial joint condyle might be one of the first human body parts to be replaced with the use of stem cells. Research on that topic might also lead to clues concerning the production of more complex organs, like the liver or the kidney (Mao, 2005).

Table 1: Comparison of complications of current therapies for synovial joint repair with stem-cell-based synovial joint condyle

Complication type	Current therapies	Stem cell based therapies
<i>Morbidity</i>	Donor site ¹	Minimal
<i>Supply</i>	Limited (autologous tissue)	Highly expandable
<i>Immunorejection</i>	Yes ²	No (from autologous stem cells)
<i>Mechanical features</i>	Wear and tear, debris ³	Anticipated to integrate with patients
<i>Pathogen transmission</i>	Yes ⁴	No (from autologous stem cells)
<i>Function</i>	Repair	Regeneration
<i>Life span</i>	Limited	Unlimited (remodeling with existing tissue)

¹ Autologous bone and cartilage grafts

² Implantation of foreign tissues

³ Refers to metals and synthetic materials

⁴ Foreign tissues

(Mao, 2005)

2.2. Cell Labeling with MRI Contrast Agents

2.2.1. Overview

Molecular imaging is defined as “the in-vivo characterization and measurement of biological processes at the cellular and molecular level” (Weissleder, 2001). Diseases cause molecular changes that can be imaged and quantified earlier than the resulting structural alterations of the affected organ. This may permit an earlier diagnosis, initiate earlier treatment and, finally, improve prognosis. For example, molecular changes in cancer cells can be detected up to 6 years before the tumor is apparent on conventional imaging studies. In order to detect malignant cells, specific contrast agents combined with ligands that selectively bind to cell surface markers, are applied (Grimm, 2003; Hengerer, Mertelmeier, 2001).

For the improvement of stem cell-based therapies, it is necessary to track the biodistribution and migration of implanted hMSCs non-invasively to make dislocations or defects of the cells visible at an early stage. This is mainly done by detecting labelled cells via radioisotope imaging, optical imaging, and MRI.

Radioisotope imaging techniques comprise planar scintigraphy, PET and SPECT. These methods are highly sensitive and enable quantification, but they have a lower resolution than MRI and CT (1 to 2 mm). Also, the toxicity of radioisotopes on stem cells has to be considered. Currently, PET and SPECT are the most widely used instruments in clinical molecular imaging applications (Grimm, 2003).

Optical imaging, including fluorescence imaging and bioluminescence imaging, provides a high sensitivity, but limited anatomical resolution and anatomical background information. It is an easy method with regard to probe synthesis and use of proteins that are self-fluorescing. A disadvantage of optical imaging is the fact that almost only superficial structures can be made visible. Also, there is the problem of autofluorescence of proteins in the body that cause interferences.

MRI is well suited for an in vivo cell tracking due to its high anatomical resolution and high soft tissue contrast. MRI contrast agents, in general, have the advantage of being less toxic than radioactive and fluorescence markers. In order to visualize transplanted stem cells, selective, cell-specific contrast agents are required (Daldrup-Link et al., 2004; Daldrup-Link et al., 2005).

MRI contrast is achieved by differences in the relaxation times of tissue water protons. Based on this principle, a number of MRI contrast agents has been developed. Gadolinium chelates and iron oxide nanoparticles have been previously applied for cell labeling and cell tracking (Grimm et al., 2003; Frank et al., 2003; Geninatti Crich et al., 2006).

2.2.2. Gadolinium Chelates

Gadolinium-based contrast agents are the standard contrast agents, currently used in clinical applications. These contrast agents are paramagnetic chelates of gadolinium, e.g. Gd-DTPA and Gd-DOTA. They shorten the T1 relaxation time of target organs, resulting in an increase of signal intensity on T1-weighted MR images. In high concentrations, Gd-chelates also shorten the T2 relaxation time of target organs, resulting in a decrease in signal intensity on T2-weighted MR images. Such high concentrations have remarkably toxic side effects, though. However, Gd-chelates are less suited for cell labelling due to their relatively low signal yield compared to iron oxides (Engström et al., 2006; Geninatti Crich et al., 2006).

Gadolinium-containing contrast agents have harmed tissues, e.g. caused arrhythmias in animal hearts (Akre et al., 1997). Due to the high toxicity of Gadolinium, the element is combined with diethylenetriaminepentaacetic acid (DTPA). The resulting Gd-DTPA complex is very stable, hydrophilic, and non-toxic (Rummeny, 2006).

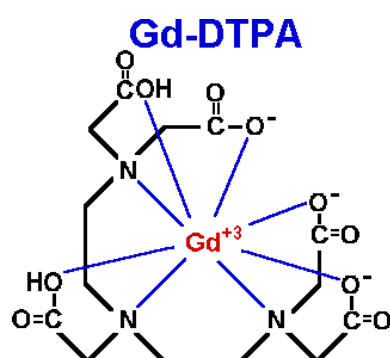


Figure 1: Chemical structure of Gadolinium-DTPA (Hornak, 1996-2004)

Several new Gd-based contrast agents with an increased r1-relaxivity have been applied for cell labeling, such as metallofullerenes, gadophrin and gadofluorine.

- Metallofullerenes are metals and metal clusters encapsulated in fullerenes, a new group of carbonaceous nanomaterials (Fatouros et al., 2006).
- Gadophrin-2 is porphyrin-based and acts as a fluorescent dye and T1 contrast agent at the same time. A fluorescing porphyrin ring surrounds two covalently linked gadolinium chelates (Daldrup-Link et al., 2004).
- Gadofluorine (Schering) is a paramagnetic gadolinium-based T1 contrast agent that is amphiphilic, i.e. lipophilic and water-soluble. It can be used to label cells by simple incubation, since it can penetrate the lipophilic membrane of stem cells (Misselwitz et al., 1999; Stoll et al., 2006). In recent studies, human monocytes have been successfully labeled

with Gadofluorine M (Henning et al., 2007). However, it has been shown that free gadolinium and gadolinium chelates both possess toxic side effects. Consequently, they can limit proteoglycan synthesis as well as cell proliferation and cause apoptosis in articular chondrocytes (Greisberg et al., 2001).

2.2.3. Iron Oxide Nanoparticles

Iron oxide nanoparticles are composed of a water insoluble magnetic core, usually magnetite (Fe_3O_4) or maghemite ($\gamma\text{-Fe}_2\text{O}_3$), with a size in the range from 4 to 10 nm. The iron oxide core is surrounded by a stabilizing dextran or starch derivative coat, which prevents an in-vivo aggregation or metabolization. As each particle contains thousands of iron atoms and the MR technique is very sensitive to these iron oxide particles, very low iron oxide concentrations can be detected with the MR technique. Iron oxides are T2 contrast agents, which mainly shorten the T2 proton relaxation time, resulting in a decrease in signal intensity on T2-weighted MR images.

The metabolism of iron oxides in humans has been well characterized. The dextran coat is cleaved in the lysosomes by dextranase and eliminated via the kidneys. The iron core is incorporated into the body's iron metabolism, such as hemoglobin within red cells. It can also be used for other iron metabolic pathways (Engström et al., 2006; Grimm, 2003; Rummeny, 2006; Reiser, 1997).

Based on their size, SPIO (superparamagnetic iron oxides) and USPIO (ultrasmall superparamagnetic iron oxides) are differentiated. SPIOs are defined by a particle diameter of more than 50 nm. Examples are ferumoxides (Endorem/Feridex) and ferucarbotran (Resovist). USPIOs are defined by a particle diameter of less than 50 nm. Examples are ferumoxtran-10 (Sinerem, Guerbet), SHU555C (Resovist S, Schering), and ferumoxytol (Advanced Magnetix).

SPIOs are primarily phagocytosed by macrophages in the liver and spleen after intravenous injection and, thus, are applied in patients as liver specific contrast agents, which permit the detection and characterization of focal liver lesions. SPIOs are T2 contrast agents.

(Simon et al., 2006; Chin, 2004; Weissleder et al., 2001; Rummeny, 2006)

USPIOs are well-suited as contrast agents for the detection of tumor manifestations in lymph nodes and the bone marrow, where they are phagocytosed by macrophages.

Recently, USPIOs have been applied in examinations of CNS inflammations and tumors as well as graft rejections, since mikroglia cells in the CNS and macrophages that infiltrate transplanted organs also take up USPIOs (Rummeny, 2006; Will et al., 2005). In addition, low

concentrations of USPIOs are useful for MR angiography and perfusion imaging due to their long blood half-life (Wang et al., 2001). USPIOs are T1 and T2 contrast agents.

Both, SPIOs and USPIOs, have been applied for stem cell labeling and in vivo cell tracking (Arbab et al., 2005; Frank et al., 2003; Pawelczyk et al., 2006).

2.2.3.1. Ferumoxides

Ferumoxides (Endorem, Guerbet or Feridex, Berlex) is the prototype SPIO, FDA-approved and clinically applied for the delineation of tumors in the liver. It is composed of an iron oxide core and a dextran coat. The particles have a diameter with a range from 80 – 150 nm. The r1-relaxivity is 40, and the r2-relaxivity is 160 mM⁻¹s⁻¹ at 37°C and 0.47 T. Ferumoxides is commercially available as a solution with a concentration of 11.2 mg Fe/ml.

Labeling of monocytes and macrophages with ferumoxides is possible by simple incubation. However, ferumoxides cannot be used for efficient labeling of nonphagocytic cells by simple incubation, as it cannot cross the cell membrane by itself owing to a negative electrostatic potential (Arbab et al., 2004). In order to achieve an efficient labeling of stem cells with ferumoxides, transfection techniques or electroporation have been used (Pawelczyk et al., 2006; Walczak et al., 2005). Polycationic transfection agents, like lipofectamine, poly-L-lysine (PLL) and protamine sulfate make intracellular labeling with ferumoxides possible when incubated for a long period of time (Walczak et al., 2005). Instant labeling of nonphagocytic cells with ferumoxides can be achieved by magnetoelectroporation (Walczak et al., 2005).

2.2.3.2. Ferucarbotran

Ferucarbotran (Resovist or SHU555A, Schering) is a second generation SPIO. It is composed of an 4.2 nm crystalline nonstoichiometric Fe²⁺ and Fe³⁺ iron oxide core and a carboxydextran coat. The particles have a mean diameter of 60 nm. The r1-relaxivity is 25.4, and the r2-relaxivity is 151 mM⁻¹s⁻¹ at 37°C and 0.47 T. Ferucarbotran was supplied to us as a solution with a concentration of 27.9 mg Fe/ml. It has been successfully applied in liver imaging in Europe since 2001 (Reimer, Balzer, 2003).

Ferucarbotran can be used for efficient labeling of phagocytic and nonphagocytic cells, precisely macrophages, monocytes, and natural killer cells, by simple incubation (Metz et al., 2004). Ferucarbotran is admitted for clinical use in Europe. The main difference between ferumoxides and ferucarbotran is the type of dextran coat. Ferucarbotran is incorporated spontaneously due to its carboxylic side groups, that ensure hydrophilic properties and enable cellular uptake (Mailänder et al., 2006). The dextran coat also prevents cells from aggregation

and metabolization. After cellular uptake, the iron oxide particle undergoes intracellular degradation in endosomes and lysosomes (Metz et al., 2004).

Table 2: Comparison of Characteristics of Resovist and Endorem

trade name	Resovist	Feridex/Endorem
generic name	Ferucarbotran	Ferumoxides
coat	carboxydextran	dextran
charge	anionic (more carboxyl groups)	neutral
cellular uptake via simple incubation	highly efficient	lowly efficient
size	60 nm	80-150 nm
contrast effect	T2/T1, predominantly negative enhancement	T2, predominantly negative enhancement
relaxivity	$r_1=25.4$, $r_2=151$ (37°C, $B_0=0.47T$)	$r_1=40.0$, $r_2=160$ (37°C, $B_0=0.47T$)
pharmacokinetics	blood pool agent, phagocytosis by RES cells after i.v. injection	RES-directed
iron concentration	28 mg Fe/ml	11.2 mg Fe/ml
dose in patients	less than 60 kg=0.9 ml more than 60 kg=1.4 ml	0.05 ml/kg
dose for cell labeling	100 µg/ml medium	50 µg/ml medium

(Mailänder et al., 2006 ; Ittrich et al., 2005 ; Wang et al., 2001 ; Arbab et al., 2004)

2.2.4. Cell Labeling Techniques

Cell labeling techniques comprise simple incubation, receptor mediated uptake, electroporation, and transfection.

Simple incubation

Cells capable of phagocytosis can be labeled by simple incubation with iron oxide particles. Examples for i.v. applications include cells of the RES, which consists of phagocytic cells located in reticular connective tissue, primarily macrophages, Kupffer cells of the liver, and tissue histiocytes. Monocytes have been successfully used for in vitro cell labeling (Oude Engberink et al., 2007).

In general, nonphagocytic cells, like hMSCs, do not take up the nanoparticles efficiently unless exposed to high iron concentrations (Sun et al., 2005; Raynal et al., 2004). In a study comparing the intracellular uptake of SPIOs and USPIOs, it was found that the uptake depended on incubation time and dose. Compared with methods using transfection agents, higher iron oxide concentrations were necessary for efficient labeling (Sun et al., 2005).

Receptor mediated uptake

A number of methods has been developed to label nonphagocytic cells with iron oxides, such as the conjugation of antigen-specific monoclonal antibodies or short HIV-transactivator transcription (Tat) proteins to the dextran coating in order to facilitate the cellular uptake (Sun et al., 2005; Arbab et al., 2003; Lewin et al., 2000). However, there is the danger of internalized peptides and antibodies inducing apoptosis or altering the biological function of some cell types (Sun et al., 2005).

Targeted imaging can be done by directing a contrast agent to particular receptors in vitro and in vivo. Iron oxide nanoparticles can be coupled to transferrin, which is taken up by the cell via endocytosis through the transferrin receptor (Grimm et al., 2003). Arabinogalactan- or asialofetuin-coated iron oxides are directed solely to hepatocytes in order to detect focal liver lesions. Monoclonal antibodies to carcinoembryonic antigen, epidermal growth factor receptors, human glioma cell-surface antigen, and other antigens combined with iron oxides have been used for tumor imaging (Wang et al, 2001).

Electroporation

Electroporation is a technique that induces reversible electromechanical permeability changes in cell membranes. Electrodes are placed close to a cell and the application of a strong electric field results in the formation of pores inside the cell membrane (Fox et al., 2006). This allows DNA or particles in the surrounding solution to enter the cell cytoplasm.

Electroporation is used to label robust and hard-to-transfect cell types, such as certain tumor cells and hematopoietic cells. Electroporation of cells could be a promising new way of intracytoplasmic iron oxide labelling of robust cell types, because it is fast, easy, and efficient (Walczak et al., 2005). One clear disadvantage of this method is the harm done to cells at high voltages or pulse durations (Walczak et al., 2005).

Transfection

Transfection describes the introduction of foreign material into cells. Transfection agents are electrostatically charged macromolecules ordinarily used for nonviral transfection of DNA into the nucleus (Arbab et al., 2003). This technique can also be used to label cells with contrast agents.

For cell labeling with contrast agents, it is not desired to deposit the contrast agent into the cell nucleus, because the contrast agent could interact with the DNA. For cell labeling, the contrast agent should be stored in secondary lysosomes within the cytoplasm of the cell. Transfection techniques for labeling of cells with contrast agents have been developed or adapted from original DNA-transfection protocols.

Polycationic transfection agents, which have been used for cell labeling, are cationic liposomes, dendrimers or PLL (poly-L-lysine) (Arbab et al., 2003; Frank et al., 2003).

Contrast agent-transfection agent complexes are incubated with the cells, traverse the cell membrane via fluid-phase endocytosis and are subsequently incorporated within endosomes (Arbab et al., 2005). Such labelled cells can be detected by MRI.

Most polycationic transfection agents are not approved by the FDA (US Food and Drug Administration), as they have significant disadvantages like cell toxicity and the formation of large complexes. Also, it is possible that complexes remain on the surface of the cells or clump cells together (Arbab et al., 2004). Recently, protamine sulfate, a low molecular weight (about 4000 Da), naturally occurring polycationic peptide, has been used as a new type of transfection agent.

Protamine sulfate is FDA approved as an antidote to heparin anticoagulation, well-tolerated by cells, and about 100 times more efficient than PLL as a transfection agent. Studies have shown that labeling of cells with iron oxide-protamine sulfate (FePro) complexes did not have

an effect on the viability and functionality of hematopoietic stem cells and mesenchymal stem cells (Arbab et al., 2005). However, other studies did in fact show adverse effects on mesenchymal stem cells labeled with PLL-coated ferumoxides, that is an inhibition of chondrogenesis (Kostura et al., 2004).

2.3. Differentiation of hMSCs

2.3.1. Overview

In the early 1980s, a series of cell lines derived from mouse bone marrow were successfully differentiated *in vitro* into adipocytes, endothelial-like cells, fibroblastoid cells and cells with fibroendothelial features. This discovery motivated for further research in that direction (Zipori, 2004).

Subsequently, it was confirmed that mesenchymal stem cells, which are located in the human bone marrow next to hematopoietic stem cells, have the capability to differentiate *in vitro* to osteoblasts, adipocytes, chondrocytes, and myocytes (Dennis et al., 2002).

Similarly to mesoderm-derived cell lines, MSCs are also capable of giving rise to bone marrow stromal cells, which in turn support hematopoietic cell growth by providing essential signaling molecules, such as granulocyte and macrophage colony-stimulating factors (G-CSF, GM-CSF, and M-CSF), Kit-ligand, IL6, fetal liver kinase (FLK)-2 ligand, and leukemia inhibitory factor (LIF) (Rafii et al., 1997).

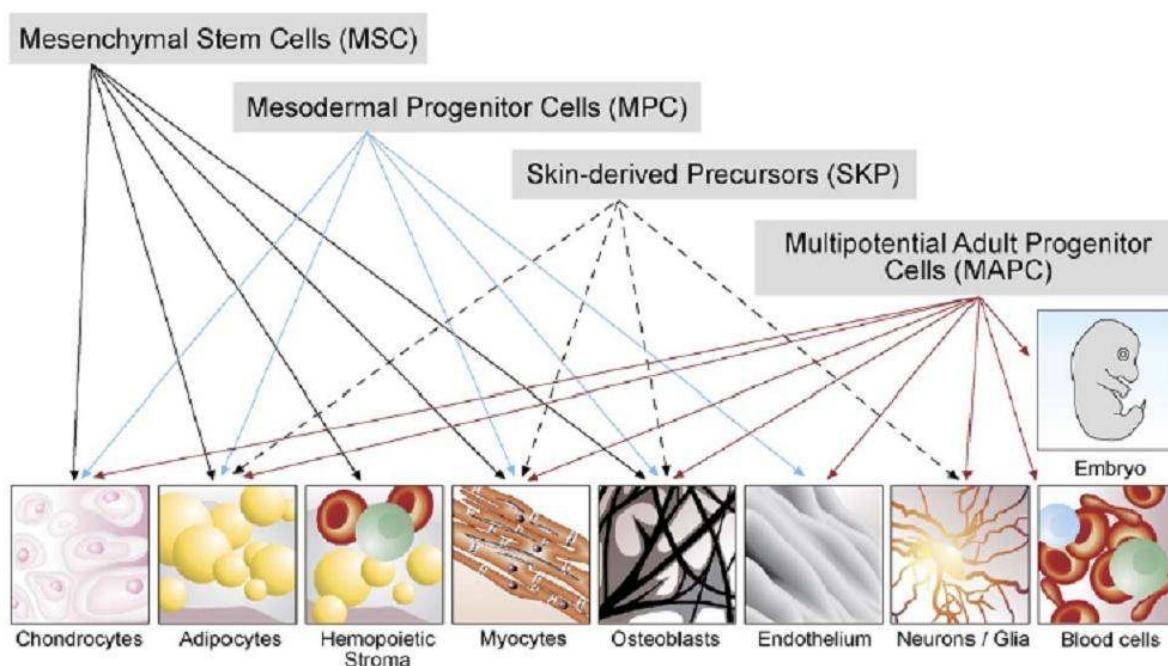


Figure 2: Differentiation Directions of Stem Cells from bone marrow and other organs (Zipori, 2004)

Several conditions are required for a successful differentiation of stem cells. To direct cells towards a certain pathway of differentiation, polypeptide growth factors and cytokines, as well as the matrix and the density of the cells, play a role (Jaiswal et al.). Furthermore, mechanical forces can have an impact on the type, timing, and extent of differentiation into tendon, cartilage, or bone tissue. In addition, specific signal transduction pathways, like protein kinases, control MSC differentiation. On the other hand, blocking of these signaling pathways causes the shift to another cell fate, a process called trans-differentiation. For example, the inhibition of the MAP kinase, which is necessary for osteogenic differentiation, results in the differentiation into adipocytes (Jaiswal et al.).

Further, it has been described that MSCs express a large variety of genes at a low level before they differentiate, allowing them to be directed towards several different pathways of differentiation. Mature cells, on the contrary, express fewer genes, but some on a higher level. This is the molecular basis for the standby-state of mesenchymal stem cells. It needs to be better understood to create a mesenchymal fingerprint, which would help to control the differentiation of MSC (Marshak; Zipori, 2004; Tuan et al., 2003; Jorgensen et al., 2004).

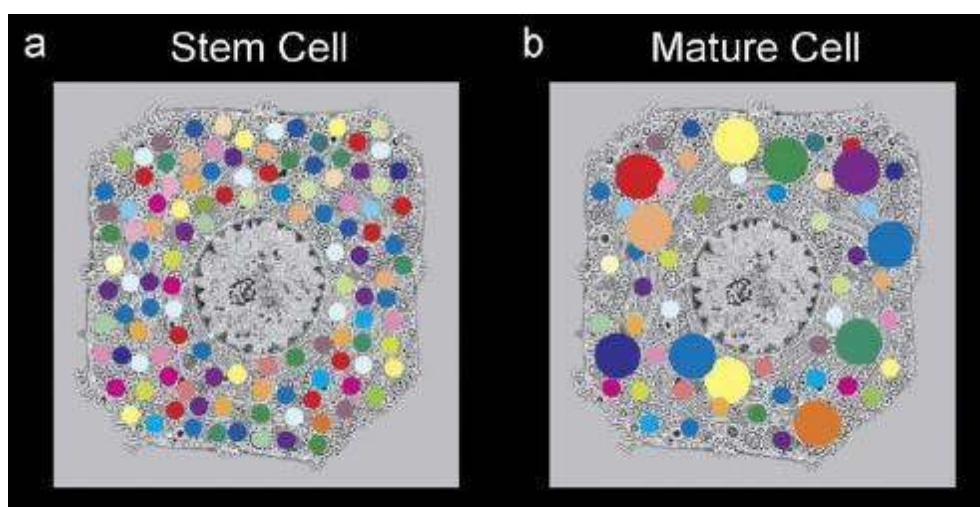


Figure 3: Gene Expression Pattern of Mesenchymal Stem Cells (Zipori, 2004): MSCs express a large variety of genes at a low level. Mature cells express fewer genes, but some on a higher level.

2.3.2. The Chondrogenic Pathway

Culture systems

Two culture systems have been developed for the chondrogenic differentiation of human mesenchymal stem cells:

The “pellet” culture system and the “alginate bead” culture system. Originally, pellet cultures were used to prevent the phenotypic modulation of chondrocytes, and alginate beads were used to maintain encapsulated cells as their differentiated phenotype.

In current studies, the pellet culture is the most commonly applied system to investigate chondrogenic differentiation. Cell aggregates emerge after a simple one-step centrifugation. The resultant pellets allow the formation of interactions in between cells, so that the culture system resembles the arrangement of chondrocytes during embryonic development (Lee et al., 2004; Johnstone et al., 1998).

Alginate is a carrier with the appropriate physical characteristics and handling properties to both promote chondrogenic differentiation by supporting the cells and to fill full-thickness osteochondral defects in vivo (Yang et al., 2004). Alginate beads induce freshly isolated articular chondrocytes to produce an extracellular matrix typical for cartilage. Furthermore, dedifferentiated chondrocytes cultured in alginate beads have been shown to return to the chondrogenic pathway (Yang et al., 2004).

Growth factors

To induce chondrogenic differentiation of human mesenchymal stem cells, a defined culture medium with certain bioactive factors, is required. Various signaling molecules that coordinate cartilage formation during skeletal development have been defined and successfully used in vitro to guide MSCs into the chondrogenic pathway.

Growth factors of the transforming growth factor- β (TGF- β) family play a crucial role in bone and cartilage development. Studies have demonstrated TGF- β 1 to stimulate the expression of certain extracellular matrix proteins typical for cartilage. However, isoforms of TGF- β 1 (TGF- β 2 and TGF- β 3) have been shown to be even more effective in enhancing chondrogenesis, as they cause a greater accumulation of extracellular proteins. Commonly, transforming growth factor is used in combination with dexamethasone to promote in vitro chondrogenesis (Mwale et al., 2006; Toh et al., 2005).

Insulin-like growth factor (IGF)-1 and two other members of the TGF- β family, that is bone morphogenetic protein (BMP)-2 or 6, and growth differentiation factor (GDF)-5, are further

factors that lead to extracellular matrix synthesis by MSCs. BMP-2 can even cause MSCs to undergo a hypertrophic development. BMP-2 and TGF- β 1 have a synergistic effect on the chondrogenic differentiation of hMSCs (Toh et al., 2005). Fibroblast growth factor (FGF)-2 is used to facilitate the proliferation and to prolong the lifespan of MSCs as well as to promote chondrogenesis (Lee et al., 2004; Toh et al., 2005; Im et al., 2006; Indrawattana et al., 2004).

By the means of BMP or FGF receptors a Smad or mitogen-activated protein (MAP) kinase is activated, which results in the expression of specific transcription factors, e.g. Sox9, the first factor to be identified, or Brachury, both having an impact on differentiation into chondrocytes. Aforesaid factors induce certain genes, such as those responsible for aggrecan and collagen II production (Jorgensen et al., 2004).

Generally, the proper combination of growth factors has been described as the key for chondrogenic differentiation (Im et al., 2006). All mentioned substances have to be further studied with regard to side effects before in vivo-use is possible. Also, the proper dose of growth factor needs to be pointed out. Too high concentrations of TGF- β 2 suppressed the proliferation of hMSCs, for example (Im et al., 2006).

Table 3: Growth factors

growth factor	characteristics	receptors	reference
dexa-methason	synthetic member of the glucocorticoid class of hormones	Intracellular - transcription factors	Johnstone et al., 1998
	antiinflammatory and immunosuppressant		Mwale et al., 2006
	potency about 40 times that of hydrocortisone		
TGF	causes oncogenic transformation: the growth of cells is no longer inhibited by the contact between cells	single pass serine/ threonine kinase	Toh et al., 2005; Im et al., 2006; Johnstone et al., 1998; Indrawattana et al., 2004; Mwale et al., 2006
IGF	polypeptides with high sequence similarity to insulin	tyrosine kinase	Indrawattana et al., 2004
	secreted by the liver as a result of stimulation by growth hormone		Im et al., 2006
	promotion of cell proliferation and inhibition of apoptosis		
	synthesis of inhibitory (IGFBP-3) and stimulatory (IGFBP-5) binding proteins to modulate the activity		Kiepe et al., 2005
FGF	involved in wound healing		Im et al., 2006
	promotes endothelial cell proliferation and angiogenesis		

growth factor	characteristics	receptors	reference
BMP	belongs to the TGF- β superfamily of proteins	specific receptors on cell surface	Kingsley, 1994
	<i>BMP-2</i>		Toh et al., 2005
	induces bone and cartilage formation		
	<i>BMP-6</i>		Indrawattana et al., 2004
	plays role in joint integrity in adults		
	plays key role in osteoblast differentiation		
collagen II	main protein of articular cartilage; enhances GAG synthesis		Bosnakovski et al., 2006, Chen et al., 2005
MIA	chemotactic factor on the mesenchymal stem cell line; influences action of BMP-2 and TGF- β 3		Tscheudschilsuren et al., 2006

Cartilage markers

To detect chondrogenic differentiation, the presence of chondrocyte specific extracellular matrix (ECM) proteins is examined by histological dyes, immunohistochemistry, or genetic analysis. Dyes like safranin-O or alcian blue are used to stain mainly glycosaminoglycans (GAG), a component of proteoglycans, secreted by chondrocytes. By combining antibodies to certain ECM proteins with fluorescence markers like diaminobenzidine (DAB) or fluorescein isothiocyanate (FITC), ECM proteins can be made visible. The expression levels of chondrocyte specific genes are measured by quantitative “Real Time” (RT)-PCR and in situ hybridization, for example (Bosnakovski et al., 2005; Tscheudschilsuren et al., 2006; Johnstone et al., 1998).

Growth factors induce the expression of type I, II, and X collagen as well as the accumulation of proteoglycans during chondrogenic development. These proteins are the main components of cartilage ECM and are to a great extent responsible for its biomechanical features, i.e. its great compressibility (Toh et al., 2005). Hyaluronan acid (HA) retains and organizes proteoglycan within the cartilage matrix. CD44, the HA-receptor, is a further proof of chondrogenic differentiation (Rousche, Knudson, 2002).

Collagen II in particular also proves to act as a growth factor, as chondrocyte specific genes are upregulated by its presence in the extracellular matrix. Type X collagen is normally used as a marker of late stage chondrocyte hypertrophy, an evidence for endochondral ossification (Bosnakovski et al., 2005; Mwale et al., 2006).

Additional cartilage markers include aggrecan, cartilage oligomeric protein (COMP), glyceraldehyd-3-phosphate-dehydrogenase (GAPDH), and melanoma inhibitory activity (MIA), also referred to as cartilage-derived retinoic acid-sensitive protein (CD-RAP). The function of MIA in cartilage tissue is not yet understood, but it has been shown on the one hand that it is secreted by cartilage cells and on the other hand that it increases the effect of BMP-2 and TGF- β 3 on chondrogenic differentiation (Lee et al., 2004; Rousche, Knudson, 2002; Tscheudschilsuren et al., 2006).

Table 4: Detection of the differentiation

cartilage marker	special feature	reference
collagen I		Im et al., 2006
		Toh et al., 2005
collagen II	also acts as a growth factor	Indrawattana et al., 2004
		Im et al., 2006
		Toh et al., 2005
		Johnstone et al., 1998
		Mwale et al., 2006
collagen X	marker of ossification	Johnstone et al., 1998
		Mwale et al., 2006
aggrecan		Indrawattana et al., 2004
		Mwale et al., 2006
GAG		Toh et al., 2005
COMP		Im et al., 2006
GAPDH		Rousche, Knudson, 2002
MIA	increases the effect of BMP-2 and TGF- β 3 on chondrogenic differentiation	Tscheudschilsuren et al., 2006
CD44		Rousche, Knudson, 2002

3. Material and Methods

3.1. Human Mesenchymal Stem Cells

Human mesenchymal stem cells (hMSCs) obtained from Cambrex and derived from a 20 year old black male's bone marrow, which tested negative for sterility, mycoplasma, hepatitis B and C and HIV, were used in this study. The hMSCs expressed CD105, CD166, CD29 and CD44, but were negative for CD14, CD34 and CD45. Furthermore, they were proven to be able to differentiate into adipogenic, chondrogenic, and osteogenic lineages.

Cultures of hMSCs were seeded at a density of 5000-6000 cells per cm², in high-glucose Dulbecco's Modified Eagle Medium (DMEM), supplemented with 10% of Foetal Bovine Serum (FBS), and 1% of Penicillin-Streptomycin. The hMSCs were cultured at 37°C in a humidified atmosphere of 5% CO₂. Medium was changed after 4 days to remove nonadherent cells and thereafter every 3 days. After 7 days, when the cells were approximately 90% confluent, the cells were trypsinized with 0.05% Trypsin-EDTA, suspended in media and centrifuged at 400 rcf for 5 minutes. The cell pellet was resuspended in culture medium and either redistributed to new culture flasks or used for the experiments. The cells were cultured at the most for 12 to 16 passages to preclude the possibility of senescence. For further cell culture, the cells were plated at a density of 3.5*10³ cells/cm² in pretreated 150cm² cell culture flasks and cultured as monolayers in DMEM High Glucose medium to prevent contact inhibition and spontaneous differentiation. (www.cambrex.com/bioproduts)



Figure 4: HMSCs plated in cell culture flasks

3.2. Labeling of hMSCs

Cells were labeled by using three different methods: (A) simple incubation with ferucarbotran (Resovist, Schering AG, Berlin, Germany), (B) transfection with ferucarbotran and protamine sulfate (American Pharmaceutical Partners, Schaumburg, IL, USA) and (C) transfection with ferumoxides (Feridex, Berlex Laboratories, Wayne, NJ, USA) and protamine sulfate:

A) Simple incubation with Ferucarbotran

HMSCs in pretreated 225cm² cell culture flasks, plated at a density of 4.8×10^3 cells/cm² were washed with DMEM medium. Then, 75 μ l ferucarbotran (Resovist) was added to these cells in 20 ml medium per T225, corresponding to a concentration of 100 μ g Fe/ml medium. Cells were also labeled with different amounts of ferucarbotran, that is 100 μ g, 50 μ g, and 25 μ g. Two hours later, 4 ml of FCS were added to the cells in order to prevent cell death or differentiation and cells were incubated for another 18 hours. After labeling, the contrast agent containing medium was removed, the cells were washed three times with PBS (Phosphate Buffered Saline) by sedimentation, (25°C, 400 rcf, 5 min) and then resuspended in DMEM medium.

B) Cell labeling of hMSCs with Ferucarbotran and Protamine Sulfate

A labeling medium was prepared, which consisted of 31.5 ml DMEM, 10.5 ml FCS, 75 μ l ferucarbotran and 21 μ l protamine. This labeling medium was added to 1×10^6 cells in 225 cm² flasks. The cells were incubated with this labeling medium for 24 hours. As a next step, the labeling medium was removed and the cells were washed three times with PBS and 7.5 units of heparin per ml to antagonize the protamine.

C) Cell Labeling with with Feridex and Protamine Sulfate

To label human mesenchymal stem cells with ferumoxides (Endorem) and protamine sulfate, serum-free RPMI (Roswell Park Memorial Institute) 1640 medium containing 1-glutamine at 4 mM, sodium pyruvate at 1mM, and MEM non-essential amino acids was used. 100 μ g sterile ferumoxides and 4 μ g sterile protamine sulfate were added per ml medium in a test tube, which was incubated for 5 minutes, so that complexes could be formed. This labeling

medium was added to 860 000 cells in 225 cm² flasks. The cells were incubated with this labeling medium for 2 hours at 37°C and 5% CO₂.

Subsequently, an equal amount of complete medium was added, resulting in a final FePro concentration of 50:2 µg per ml, and this solution was incubated with the cells overnight.

After the medium had been removed, the cells were washed 3 times with PBS and 7.5 units of heparin per ml to improve the washing. Cells were trypsinized, centrifuged and collected then. (Arbab et al., 2004)

After labeling, samples were cultured for 2 hours, 6 days or 12 days. The so-called pre-culturing with additional washing of cells was carried out to detect any kind of influence on the viability or differentiation capacity of incubated cells.

3.3. Chondrogenic Differentiation of labeled hMSCs

The Complete Chondrogenic Induction Medium contained Differentiation Basal Medium – Chondrogenic medium, dexamethasone, ascorbate, ITS plus supplement, pen/strep, sodium pyruvate, proline and L-glutamine. The growth factor TGF-β3 was added to a final concentration of 10 ng/ml.

After washing, the labeled hMSCs were resuspended in complete chondrogenic medium to a concentration of 5 x 10⁵ cells per ml. 2.5 x 10⁵ cells in 0.5 ml medium were aliquotted into 15 ml polypropylene culture tubes. Subsequently, cells were centrifuged at 150 g for 5 minutes at room temperature, the caps of the tubes were loosened one half turn to allow gas exchange and the pellets were incubated at 37°C and 5% CO₂.

The medium in the tubes was completely exchanged every 2 days. The harvesting of the chondrogenic pellets took place after 14 days in culture. (www.cambrex.com/bioproductions)

3.4. MR Imaging and Data Analysis

MR images were obtained using a 1.5 T clinical scanner (Signa EXCITE HD 1.5 T, GE Medical Systems, Milwaukee, WI, USA; Figure 6) and a standard circularly polarized quadrature knee coil (Clinical MR Solutions, Brookfield, WI, USA). To avoid susceptibility artifacts from the surrounding air in the scans, all probes were placed in a water-containing plastic container at room temperature (20°C).

Coronal T1- and T2-weighted Spinecho (SE) sequences were obtained with varying repetition times (TR) (2000, 1000, 500, 250 ms) and varying echo times (TE) (64, 48, 32, 16 ms).

Axial T2*-weighted Gradient echo (GE) sequences were obtained with a flip angle of 30 degrees, a TR of 500 ms and varying TEs of 28, 14, 7.4 and 4.2 ms. All sequences were acquired with a field of view (FOV) of 120x120 mm, a matrix of 256x196 pixels, a slice thickness of 2 mm and two acquisitions. MR images were transferred as DICOM images to a SUN/SPARC workstation (Sun Microsystems, Mountain View, CA, USA) and processed by a self-written IDL program (Interactive Data Language by Research Systems, Boulder, CO, USA).

T1 and T2 relaxation times of the cell samples were calculated assuming a monoexponential signal decay and using a nonlinear function least-square curve fitting on a pixel-by-pixel basis. T1 relaxation times were calculated using four spin echo images with a fixed TE of 16 ms and variable TR values of 2000, 1000, 500 and 250 ms. T2 relaxation times were calculated with a fixed TR of 2000 ms and variable TE values as specified above. T2* times were calculated with a fixed TR of 500 ms and variable TE values.

Signal intensities for each pixel as a function of time was expressed as follows:

$$\mathbf{T1:} \quad M_z(t) = M_0 \cdot \left(1 - ce^{-\frac{t}{T_1}}\right) \quad \mathbf{T2 \text{ and } T2*}: \quad M_T(t) = M_T(0) \cdot e^{-\frac{t}{T_2}}$$

T1 and T2 relaxation times of free and cell bound iron oxides were derived by ROI measurements of the test samples on the resultant T1- and T2-maps, and results were converted to R1- and R2-relaxation rates [s^{-1}]. Care was taken to analyze only data points with signal intensities significantly above the noise level.



Figure 6: 1.5 T Clinical MRI-Scanner

3.5. Spectrometry

The iron concentrations of all test samples were determined by inductively coupled plasma atomic emission spectrometry (ICP-AES) (IRIS Advantage, Thermo Jarrell-Ash, MA, USA). Samples were dissolved in a microwave (400 W for 55 min) by adding 65% HNO₃ and 30% H₂O₂. The obtained solutions were nebulized into an argon plasma.

Collaborators from Schering AG Berlin, who were blinded with respect to the content of the samples, performed these analyses.

3.6. Histology

After 14 days of differentiation, the resulting pellets were examined histologically by Safranin O and Alcian Blue staining to evaluate the presence of cartilaginous matrix. Additionally, the viability of the cells and the amount of iron within the pellet, which appeared brown to gold, were judged.

After the medium had been removed, pellets were fixed in 10% Neutral Buffered Formalin (Richard-Allan Scientific). To encapsulate and retain the entire pellets during histological processing, HistoGel Specimen Medium (Richard-Allan Scientific) was used. Cells were dehydrated in a tissue processor (Tissue Tek VIP), paraffin embedded and sections at 5 μ m thickness were cut. Slides were deparaffinized in xylene and rehydrated through alcohols to water. Subsequently, the pellet sections were stained in Alcian Blue or Safranin O, to detect sulfated glycosaminoglycans.



Figure 7: Histological Staining

3.7. Glycosaminoglycan Quantification

DMMB (Dimethylmethylene Blue) assay is an absorbant assay that assesses the total GAG content in the used media. To perform a DMMB assay, all of the chondrogenic induction medium had been saved and stored at -20°C . At cell culture endpoint, pellets were digested in $450\ \mu\text{l}$ of papain solution overnight at 60°C .

Two standard dilution series were made using values ranging from 0 to 100 $\mu\text{g/ml}$: One with chondroitin sulfate dissolved with 1X TE buffer (a commonly used buffer solution in molecular biology) and the other with chondroitin sulfate dissolved in incomplete chondrogenic medium. One 96-well sample plate with medium samples and the medium standard curves, and another with cell pellet samples and the TE buffer standard curve, were run in a microplate reader (Spectra Max M5, Molecular Devices) at OD (optical density) 525 nm. To run plates, $40\ \mu\text{l}$ standard or sample were added to $250\ \mu\text{l}$ DMMB solution (21 mg DMMB, 5 ml absolute ethanol and 2 g sodium formate; pH 3.5). Values were calculated based on the standard dilution series.

4. Results

4.1. Pellets

The rate of chondrogenic differentiation of labeled cells and unlabeled controls was evaluated qualitatively by morphological changes of the pellets over 14 days.

The control formed solid pellets from day two on, which stayed stable until day 14. This is indicative of a regular chondrogenic differentiation (Figure 8A). Pellet formation of all labeled cells was compared to the control.

Ferucarbotran-labeled cells were not capable of forming pellets, more precisely the artificially shaped pellets disintegrated from day two on (Figure 8B). The ferucarbotran-labeled, but for 6 or 12 days precultured cells, showed a greater chondrogenic potential by shaping compact pellets from day 2 on (Figures 8C and 8D). Pellets consisting of ferucarbotran/protamine-labeled or ferumoxides/protamine-labeled cells stayed compact until day 2, but disintegrated on day 5 (Figures 8E and 8G).

The 6 days preculture of ferumoxides and protamine-labeled cells resulted in a greater extent of differentiation, shown by the formation of pellets from day 3 on (Figure 8H). The ferucarbotran and protamine as well as the 6 days preculture of ferucarbotran and protamine disintegrated on day 3 (Figures 8E and 8F).

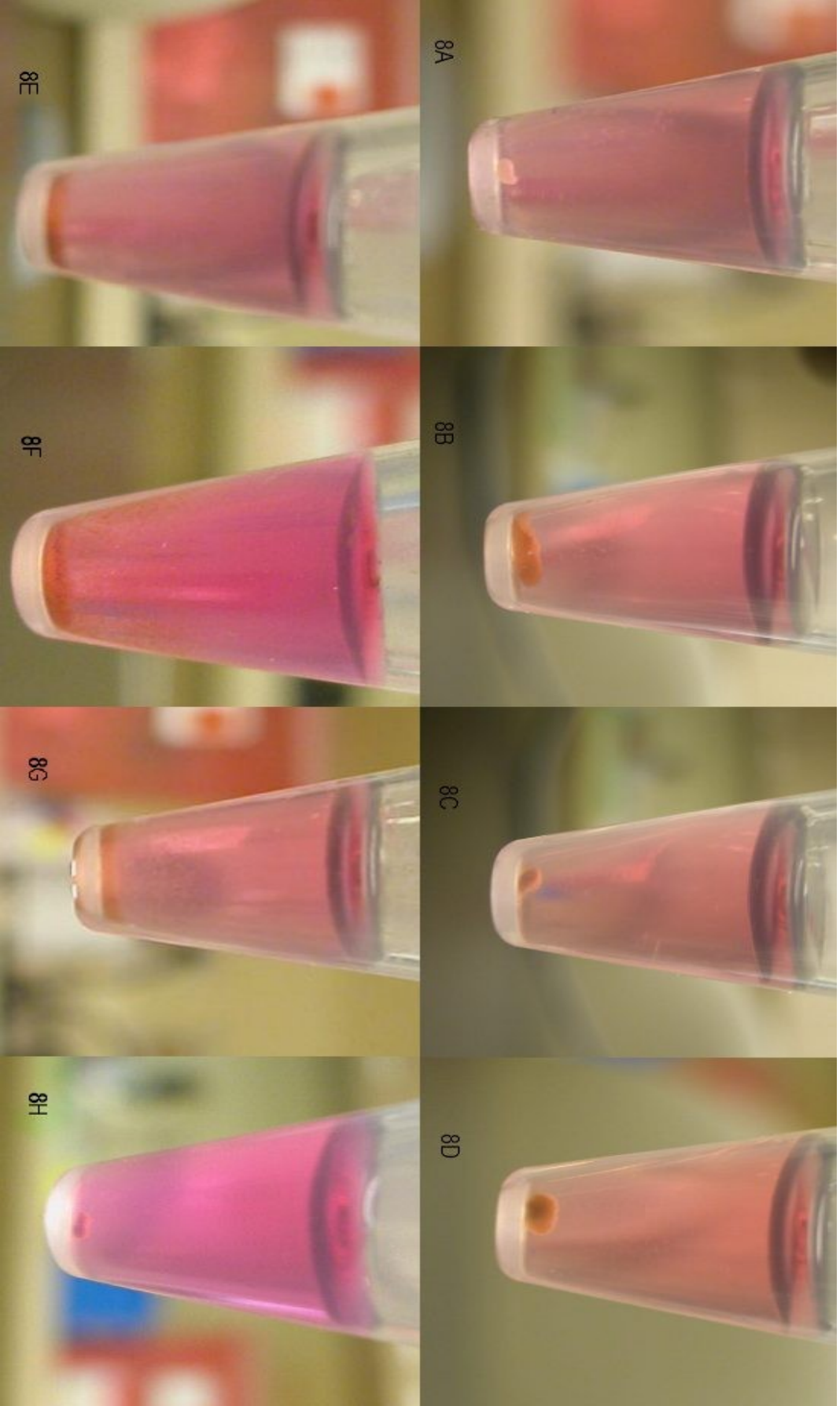


Figure 8A: Control

Figure 8B: Ferucarbotran

Figure 8C: Ferucarbotran 6 days

Figure 8D: Ferucarbotran 12 days

Figure 8E : Ferucarbotran and Protamine

Figure 8F : Ferucarbotran and Protamine 6 days

Figure 8G: Ferumoxides and Protamine

Figure 8H: Ferumoxides and Protamine 6 days

4.2. MR Imaging and Data Analysis

MR images were taken of all samples on day 14 of the differentiation to demonstrate labeling efficiency (Figure 9). Iron oxide-labeled cells cause a susceptibility artifact and appear as hypointense areas on MR images (Arbab et al., 2004; Frank et al., 2003). MR imaging of chondrogenic pellets showed a marked signal loss of labeled MSCs compared to the unlabeled controls on T2 and T2* images (Figure 9). This area of signal loss exceeded the size of the labeled cell pellets.

Compared to the control, which did not present any susceptibility artifact, the strongest effect was detected in the ferucarbotran and protamine samples. All the other samples showed a smaller susceptibility artifact than ferucarbotran and protamine, but more than the control.

In the samples that were incubated with 100 μg of ferucarbotran, the susceptibility effect was more intense than in the 50 μg and 25 μg samples and in the ferumoxides samples.

Corresponding SNR (Signal-to-Noise Ratio) values were at least 10-fold lower for all labeled cell pellets compared to the unlabeled controls (Figure 9). SNR data of labeled pellets (representing the magnitude of signal loss) were not much different for the applied T2 and T2* sequences. However, the susceptibility effects of labeled pellets (i.e. area of signal loss) were larger on T2* compared to T2-images. This corresponds to the fact that T2* sequences mainly show inhomogeneities in magnetic fields, which are caused by iron oxides, for example (Brindle et al., 2003).

MR: Pellets day 14

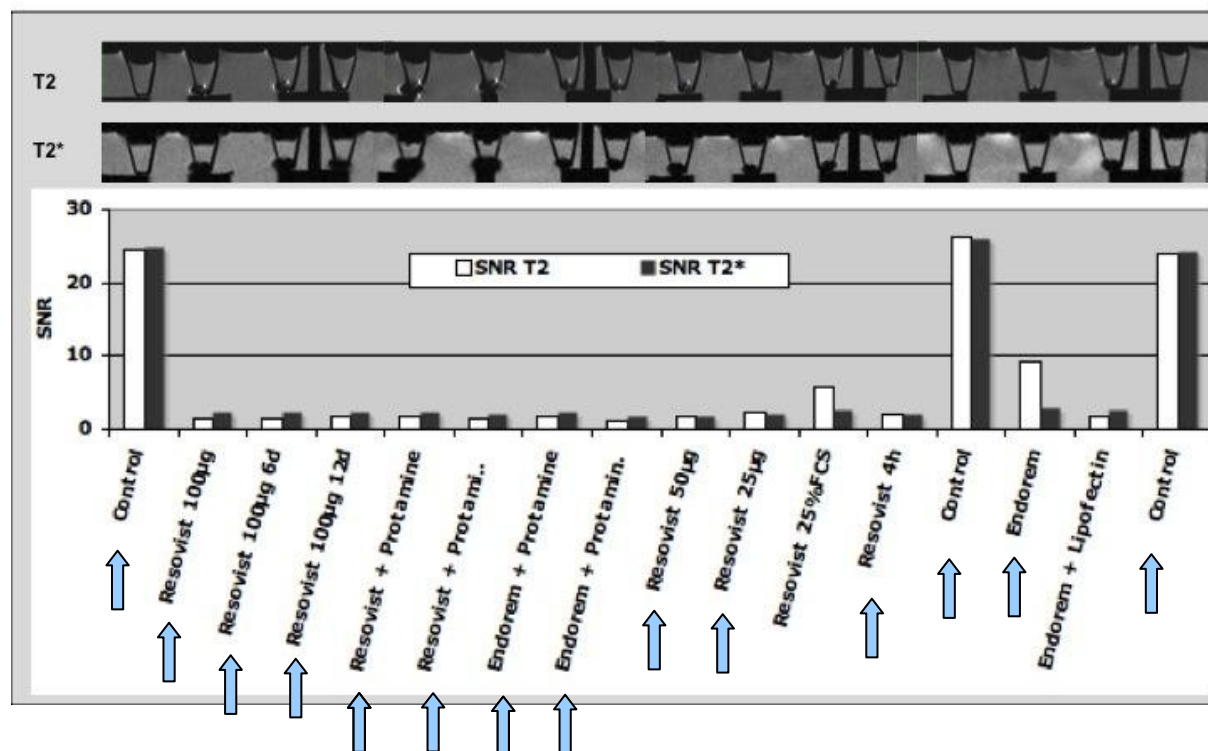


Figure 9: MR images of samples on day 14 of the differentiation

4.3. Spectrometry

Labeling efficiency was quantified by detecting the amount of iron per cell via spectrometry. The iron content was set into relation with the viability of the cells, which was judged by trypan blue stain. Applying this method, dead cells stain blue, while living cells exclude trypan blue.

Control

One control revealed 0.06 pg of mean iron per cell and a cell viability of 98%, in the other control there was no iron detected (0.0 pg) and the viability was 99%. (Figure 10A)

One control contained 0 pg of iron per cell and 98% of cells were viable. Values for the second control were 1.3 pg of mean iron per cell and 97% viability. (Figure 10B)

Ferucarbotran

Cells had been labeled with different amounts of ferucarbotran, that is 100 μg , 50 μg , and 25 μg . According to that, they contained 5.56 pg, 4.62 pg, and 2.79 pg per cell respectively. Viability was 97% for 50 μg and 25 μg of ferucarbotran, for 100 μg it was 96%.

The amount of mean iron per cell for ferucarbotran 4 hours prelabeled was 3.21 pg, the viability 96%. Ferucarbotran that was prelabeled 6 days and 12 days showed a higher viability (98%). The 6 days prelabeled cells contained 5.45 pg and the 12 days prelabeled cells 4.08 pg per cell.

Ferucarbotran without prelabeling revealed 7.08 pg per cell with a viability of 97%, and cells labeled with ferucarbotran and protamine contained 25.65 pg average iron per cell. The viability of ferucarbotran and protamine was 89%. (Figure 10A)

Ferumoxides

Ferumoxides-labeled cells revealed 3.9 pg, ferumoxides and protamine-labeled cells 8.67 pg of iron per cell. Viabilities were 98% for ferumoxides alone and 92% for ferumoxides and protamine. (Figure 10B)

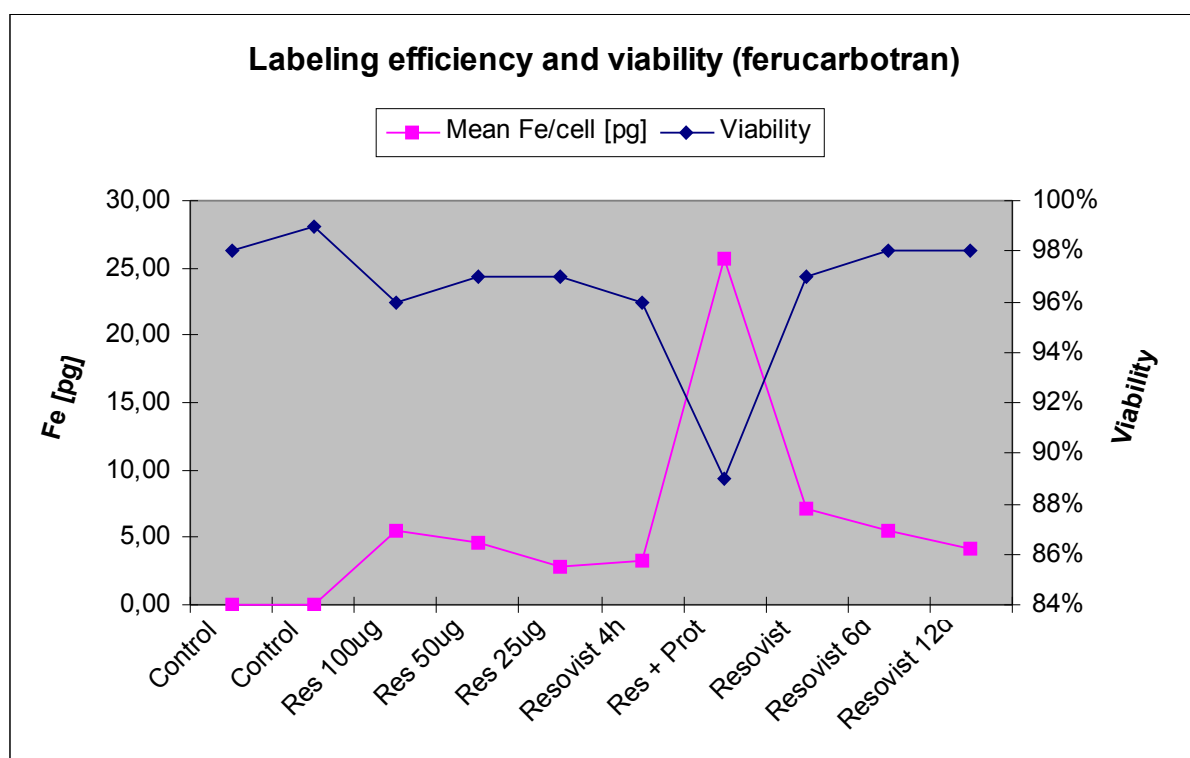


Figure 10A shows the labeling efficiency measured by the mean iron per cell and the viability judged by trypan blue stain of ferucarbotran-labeled cells

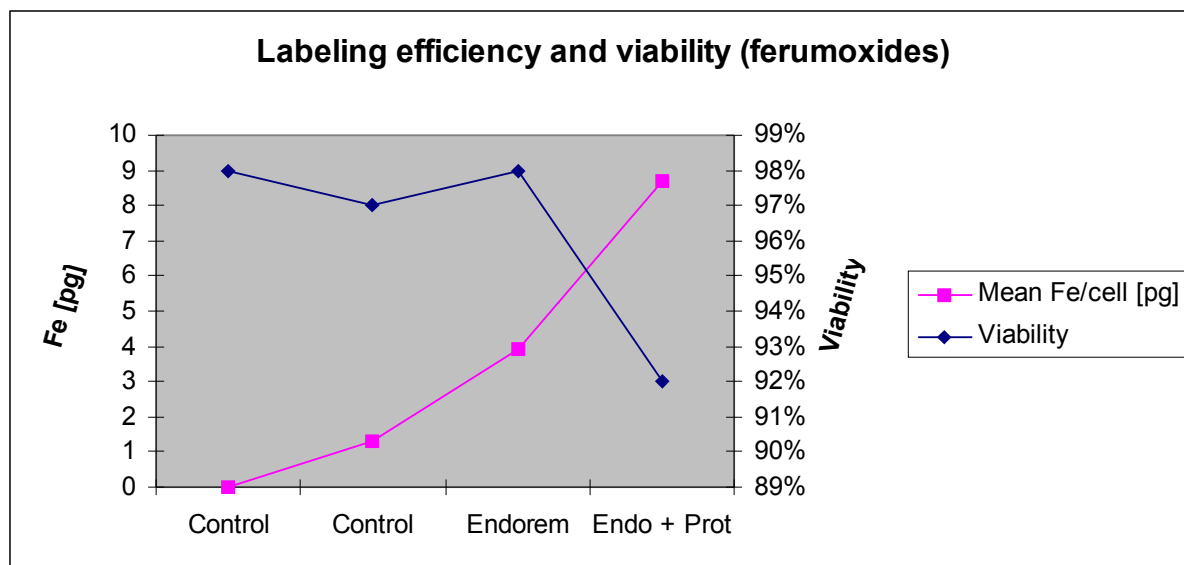


Figure 10B shows the labeling efficiency measured by the mean iron per cell and the viability judged by trypan blue stain of ferumoxides-labeled cells

4.4. Histology

4.4.1. Safranin O

The cells in the control had a morphology comparable to cartilage cells, with a considerable degree of proteoglycan deposition throughout the pellet. Round nuclei and nucleoli could be seen (Figure 11A).

The remaining slides showed an accumulation of the magnetic nanoparticles. The use of protamine as a transfection agent led to an increased iron-deposition that came along with an increased rate of apoptosis.

In the ferucarbotran- and ferumoxides plus protamine 6 days-slides the iron was detectable (Figures 11E and 11B), whereas ferucarbotran and protamine showed an iron overload (Figures 11C and 11D). The highest rate of cell death could be found in the ferucarbotran and protamine-slides (Figure 11D), followed by an also very high rate in ferumoxides and protamine 6 days (Figure 11E) and the other ferucarbotran and protamine-slide (Figure 11C). Among the ferucarbotran-labeled cells the rate of cell death was low (Figure 11B).

Ferucarbotran alone and ferumoxides and protamine (6 days preculture)-labeled cells showed an iron deposition lower than that in ferucarbotran and protamine-labelled cells, but only ferucarbotran exhibited a greater cell viability. All cells appeared to have differentiated like

the control. Slides of ferucarbotran 6 days and ferucarbotran plus protamine 6 days were made, but there were no cells detectable.

Table 5: Safranin O Staining

	description	level of differentiation	cell death	amount of iron
Control	round nuclei, nucleoli to be seen, morphology comparable with cartilage cells, spindle-like cells, cells are heading towards chondrogenic pathway	differentiation like control	hardly any	none
Fer and Prot	no pellet	no pellet	-	-
Fer and Prot 6d	iron appears brown/gold, cell death	differentiation like control	accelerated	detectable
Res	minor cell death (looks better than Fer and Prot 6d)	differentiation like control	low	detectable
Res 6d	no cells	no differentiation	-	-
Res and Prot 1	a lot of iron, few cells, not very much different from control	differentiation like control	accelerated	iron overload
Res and Prot 2	too much iron, major cell death	differentiation like control	high	iron overload
Res and Prot 6d	no pellet	no pellet	-	-

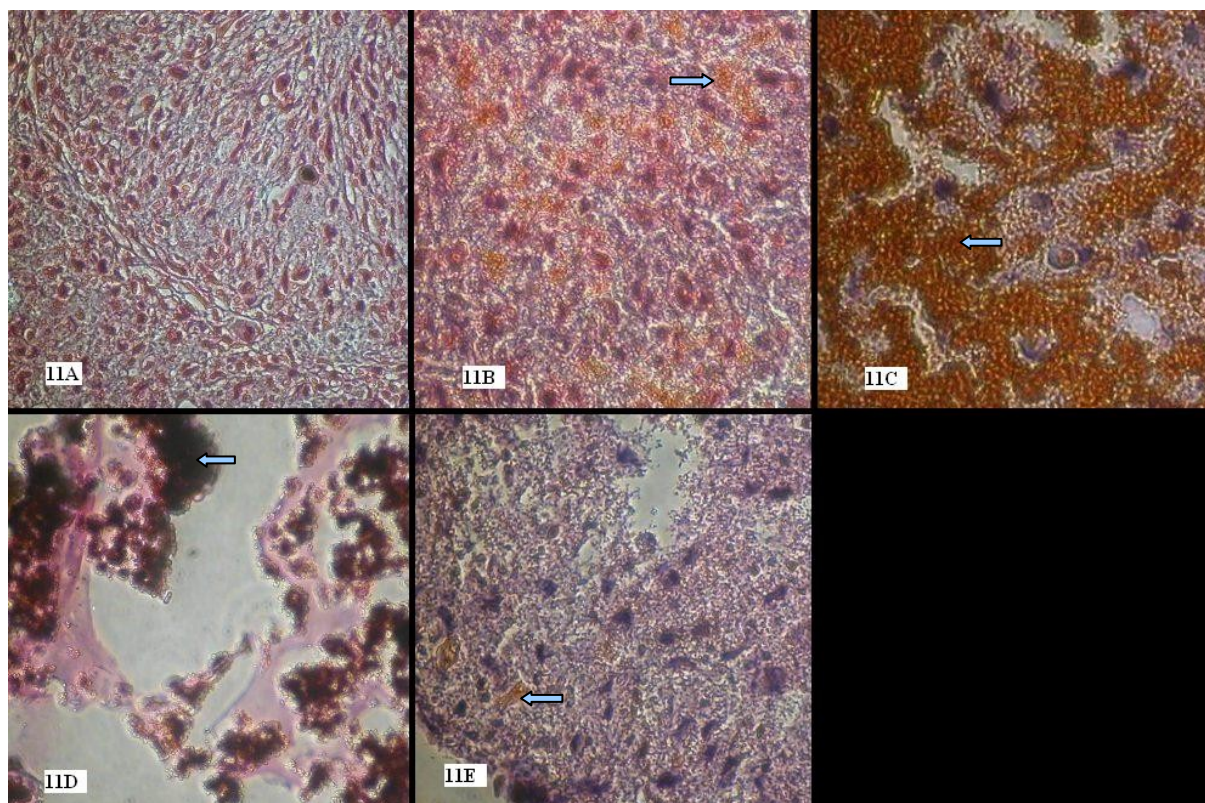


Figure 11A: Control

Figure 11B: Ferucarbotran

Figure 11C: Ferucarbotran and Protamine 1

Figure 11D: Ferucarbotran and Protamine 2

Figure 11E: Ferumoxides and Protamine 6 days

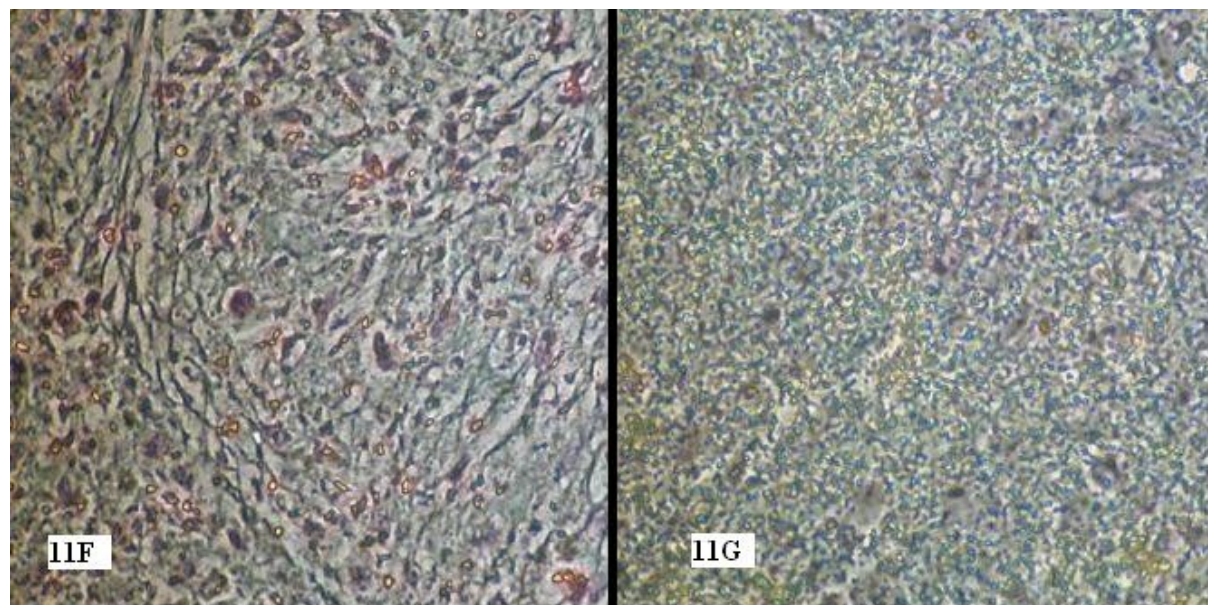
4.4.2. Alcian Blue

Alcian Blue staining normally shows glycosaminoglycans, which turn out blue. However, the color blue is only a proof of chondrogenic differentiation if it is detected intracellular, because GAG is a normal component of extracellular matrix.

In our slides, there could only be seen blue extracellular in the control and in ferumoxides and protamine 6 days (Figures 11F and 11G). The other slides did not present any blue.

Table 6: Alcian Blue Staining

	intensity of stain
Control	blue extracellular
Fer and Prot	no blue
Fer and Prot 6d	blue extracellular
Res	no blue
Res 6d	no pellet
Res and Prot 1	no blue
Res and Prot 2	no blue
Res and Prot 6d	no pellet

**Figure 11F: Control****Figure 11G: Ferumoxides and Protamine 6 days**

4.5. Glycosaminoglycan quantification

For the quantification of the chondrogenic differentiation of all samples, the total sulfated glycosaminoglycan produced by chondrogenic cells was measured (Figure 12A).

The unlabeled control, which had not been treated with iron oxide nanoparticles, revealed the highest amount of GAG, that is 25.04 μg in total, 20.87 μg in the media and 4.17 μg in the pellets.

The cells that were incubated with ferucarbotran and precultured for 12 days produced 19.0 μg over 14 days (9.5 μg in the media and 9.5 μg in the pellets). For ferucarbotran and 6 days of preculture the GAG production was 13.18 μg (8.33 μg in the media and 4.85 μg in the pellets).

Ferucarbotran and protamine-labeled cells that had been cultured for 6 days before the induction of the differentiation showed a higher level of differentiation than those without preculture, a fact that results from the production of 13.07 μg of total GAG for 6 days (7.27 μg in the media and 5.8 μg in the pellets) and 12.13 μg for no preculture (10.76 μg in the media and 1.37 μg in the pellets).

The cells incubated with ferumoxides and protamine that had been precultured for 6 days secreted 10.68 μg of GAG (7.56 μg in the media and 3.12 μg in the pellets). Ferumoxides and protamine-labeled cells that had been led to the chondrogenic pathway immediately after labeling secreted 8.77 μg of total GAG over 14 days (8.33 μg in the media and 0.44 μg in the pellets).

The least production of GAG was detected in the cells treated with ferucarbotran without additional culturing. It was 3.48 μg (2.91 μg in the media and 0.58 μg in the pellets).

The GAG-content was directly proportional to the days of prelabeling, which is shown in figure 12B.

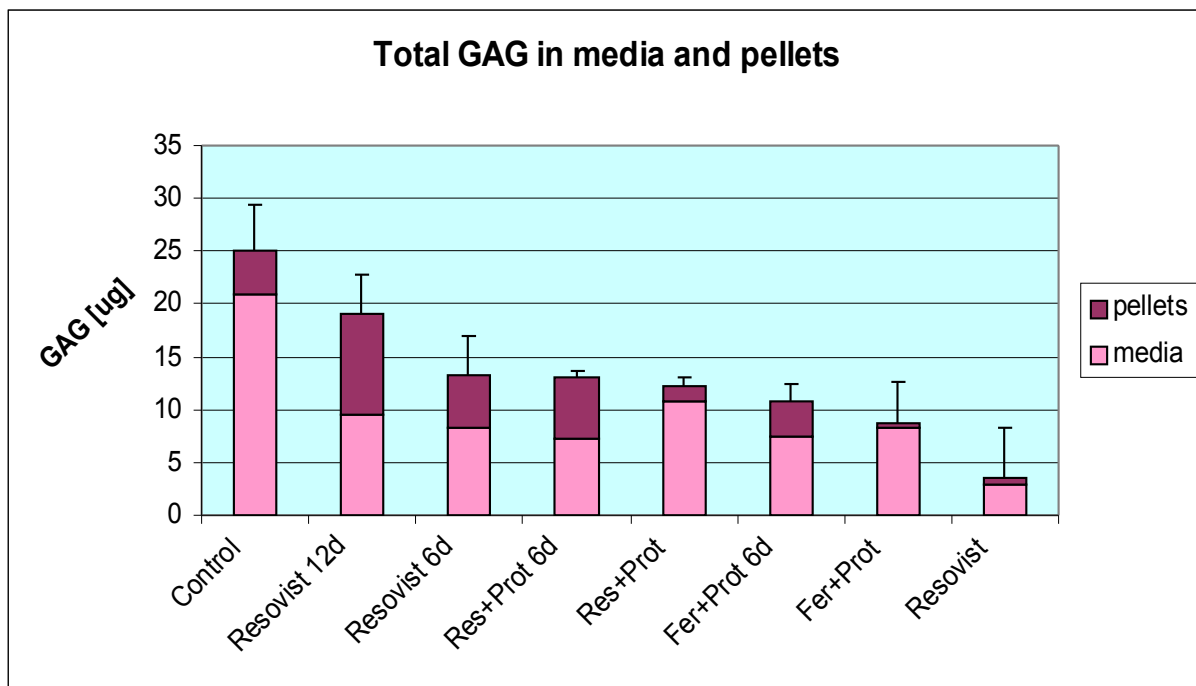


Figure 12A

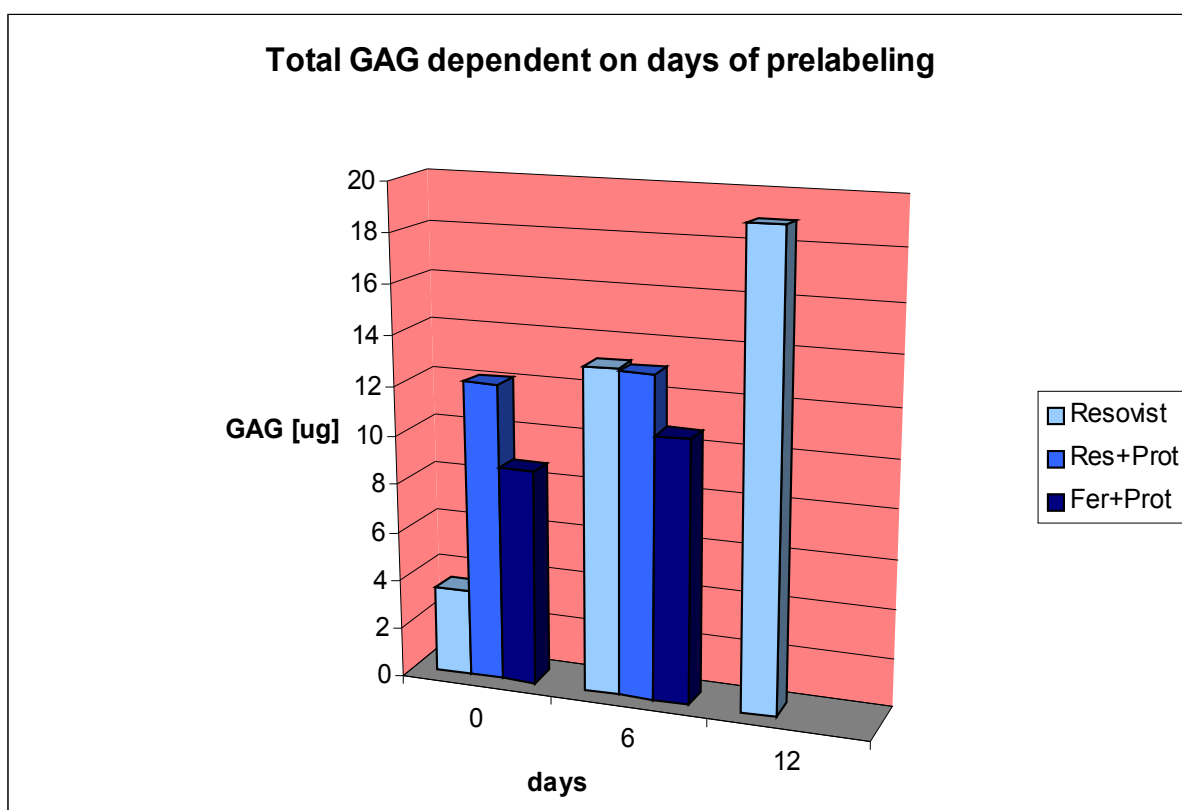


Figure 12B

5. Discussion

This study showed that magnetic labeling with ferucarbotran and ferumoxides can inhibit viability and chondrogenesis of hMSC, depending on the use of transfection agent, the concentration and the days of prelabeling.

An unimpaired viability and differentiation capacity of iron oxide-labeled hMSCs is a mandatory prerequisite for any application of stem cells for cell tracking studies. Therefore, the biocompatibility of stem cell labeling with iron oxides has to be studied precisely and a labeling protocol needs to be developed that does not significantly interfere with the cells' viability and chondrogenesis.

Our differentiation protocol demonstrated that ferucarbotran-labeled cells that had been washed and cultured for 6 or 12 days before the differentiation was induced formed solid pellets compared to the ferucarbotran-labeled cells without preculture. Thus, the prelabeling is thought to improve viability and differentiation capacity.

This complies with the findings in spectrometry. Viability correlates directly and iron content indirectly with the days of prelabeling.

Also, most glycosaminoglycans were detected in the ferucarbotran 12 days and ferucarbotran 6 days samples. Generally, the longer the time of prelabeling, the more GAG was produced.

Transfection with protamine yielded the highest iron uptake into the cell and, in this way, appeared to disturb differentiation. Ferucarbotran/ferumoxides and protamine-labeled cells did not form pellets, contained most iron and showed most cell death in Trypan Blue and Safranin O stains.

In GAG quantification, results were better for ferucarbotran and protamine than for ferumoxides and protamine, which could indicate that ferucarbotran does not disturb differentiation as much as ferumoxides. Furthermore, ferucarbotran achieved the best results in histology concerning viability.

Differentiation protocol, histology, and GAG quantification demonstrate that ferumoxides and protamine 6 days appeared to differentiate to a higher extent and to be more viable than ferumoxides and protamine, a fact that matches the findings mentioned above.

In MRI, the strongest effect was induced by ferucarbotran and protamine-labeled cells, suggesting that this is the most efficient labeling method.

Spectrometrical data showed that the amount of ferucarbotran correlates with the mean iron per cell and indirectly with cell viability.

In histological analysis none of the labeling methods seemed to interfere with the differentiation capacity, however, ferucarbotran and protamine as well as ferumoxides and protamine-labeled cells showed the highest amount of iron and most cell death.

As a conclusion, this impaired viability and differentiation of hMSCs we found may have been related to a too high quantity of internalized contrast agent into the cells.

Labeling of stem cells by ferumoxides in combination with transfection agents, such as protamine sulfate or poly-L-lysine (PLL) has been frequently documented (Arbab et al., 2003; Arbab et al., 2004; Arbab et al., 2005; Kostura et al., 2004).

However, most polycationic transfection agents (e.g. PLL) are not approved by the Food and Drug Administration (FDA), can be toxic to cells and cause significant cell death (Arbab et al., 2004).

Ferumoxides and protamine are both commercially available and FDA-approved. In former studies, ferumoxides and protamine-labeled hMSCs did not show any toxicity, changes in differentiation capacity or in the phenotype (Arbab et al., 2004; Arbab et al., 2005).

Another study showed for the first time that labeling with ferumoxides can have adverse effects on chondrogenic differentiation (Kostura et al., 2004). This was confirmed by other groups that described inhibition of chondrogenesis by magnetic labeling with the SPIO ferumoxides (Bulte et al., 2004) or an impair of the viability of stem cells when they are internalized in too high quantities into the cells (Metz et al., 2004; Daldrup-Link et al., 2003).

Recently, hMSCs have been successfully labeled with ferucarbotran, without aid of a transfection agent. This was shown to simplify the labeling procedure, to be more effective and to cause less apoptosis (Hsiao et al., 2007; Metz et al., 2004, Henning et al., 2006).

No significant change in viability, proliferation, and differentiation capacity was found (Hsiao et al., 2007).

On the one hand, these findings increase confidence that labeling with ferumoxides/protamine and ferucarbotran could in the future permit the trafficking of stem cells *in vivo*, particularly as SPIOs like ferumoxides and ferucarbotran are already widely used in the detection and differentiation of liver tumors (Reimer, Balzer, 2003).

On the other hand, results of several studies, including ours, indicate that labeling of hMSCs with ferumoxides/protamine and ferucarbotran can have an effect on the viability and differentiation capacity of the cells. First, protamine could lead to iron overload of cells, which would lead to cell death. Additional inhibition might be caused by surface bound iron deposits. It is known that chondrogenic differentiation highly depends on surface-linked

cellular interactions and needs to be conducted in a 3D culture (Mwale et al., 2006). It seems likely that surface-bound iron oxide particles could interfere with essential mechanisms or structures. This explanation is suitable with the fact that additional washing and culturing of the cells improved viability and differentiation capacity, because with every washing, iron is removed from the cell surface.

In follow-up studies, a new labeling protocol will have to be developed, in which cellular iron uptake will be limited. If applied in limited concentrations, iron oxides are slowly incorporated into the regular iron metabolism and do not change the physiology of the cells (Bos et al., 2004; Kostura et al., 2004; Bulte et al., 2004; Arbab, Yokum et al., 2004; Arbab, Yokum et al., 2005; Daldrup-Link et al., 2003).

Furthermore, iron could be made visible on the cell surface and inside the cell by fluorescence microscopy. The mechanism of differentiation inhibition also needs further investigation.

Besides, Hematoxylin and Eosin Stain could be used instead of Safranin O and Alcian Blue, because it is the most widely used stain and histologists would be more common with changes in cell morphologies as well as with colors.

In comparison to former studies, we quantified the extent of differentiation by glycosaminoglycan production, which turned out to be an efficient method.

It needs to be furtherly explored in how far prelabeling influences viability and differentiation, especially with a prelabeling-period of 12 days. Also, further studies about labeling with different amounts of ferucarbotran would provide more information on the best concentration to label hMSCs.

Before in vivo trials and clinical applications can be started, the effects of magnetic labeling on hMSCs will have to be investigated in more detail. In vivo, SPIOs are mostly phagocytosed after i.v. injection and iron content decreases after cell division, so that monitoring time of stem cells will be limited (Jung, 1995). In addition, the spatial resolution of MRI needs to be improved to track stem cells more precisely (Hsiao et al., 2007).

6. Summary

In this study, human mesenchymal stem cells were labeled with MR contrast agents and afterwards led to differentiation into chondrocytes. The aim was to detect the effects of ferumoxides/protamine and ferucarbotran-labeling on the viability and differentiation capacity of stem cells. Besides, factors like the use of protamine as a transfection agent, a period of preculturing with additional washing before differentiation and the use of different amounts of contrast agent were taken into consideration. These effects on stem cells were evaluated by documentation of morphological changes of the cells, detection of the mean iron content per cell, Trypan Blue stain to evaluate the viability, Safranin O and Alcian Blue stains to detect glycosaminoglycans, and glycosaminoglycan quantification.

For our labeling protocols, there was an anti-proportional relation between the intracellular iron oxide concentration and the rate of chondrogenic differentiation. This supports a dose-dependent inhibition of chondrogenesis. Particularly the additional use of protamine and the immediate differentiation after labeling led to cell death and limitations of differentiation, with ferucarbotran seeming to interfere less with differentiation than ferumoxides. However, using ferumoxides/protamine and ferucarbotran, hMSCs can be labeled efficiently.

7. Bibliography

1. Akre, B.T., Dunkel JA, Hustvedt SO, Refsum H, Acute cardiotoxicity of gadolinium-based contrast media: findings in isolated rat heart, *Acad Radiol* 1997, 4: 283-291
2. Alcantara, L.S., Chen J, Kwon CH, Jackson EL, Li Y, Burns DK, Alvarez-Buylla A, Parada LF, Malignant astrocytomas originate from neural stem/progenitor cells in a somatic tumor suppressor mouse model, *Cancer Cell*, 2009, Jan 6, 15(1): 45-56
3. Arbab, A.S., Wilson LB, Ashari P, Jordan EK, Lewis BK, Frank JA, A model of lysosomal metabolism of dextran coated superparamagnetic iron oxide (SPIO) nanoparticles: implications for cellular magnetic resonance imaging, *NMR Biomedicine* 2005, 18:383-389
4. Arbab, A.S., Yocum GT, Kalish H, Jordan EK, Anderson SA, Khakoo AY, Read EJ, Frank JA, Efficient magnetic cell labeling with protamine sulfate complexed to ferumoxides for cellular MRI, *Blood* 2004, Volume 104, Number 4
5. Arbab, A.S., Bashaw LA, Miller BR, Jordan EK, Bulte JW, Frank JA, Intracytoplasmic Tagging of Cells with Ferumoxides and Transfection Agent for Cellular Magnetic Resonance Imaging after Cell Transplantation: Methods and Techniques, *Brief Communications*, October 15, 2003, pp.1123-1130
6. Arbab, A.S., Yocum GT, Rad AM, Khakoo AY, Fellowes V, Read EJ, Frank JA, Labeling of cells with ferumoxides-protamine sulfate complexes does not inhibit function or differentiation capacity of hematopoietic or mesenchymal stem cells, *NMR Biomedicine* 2005,18:553-559
7. Barry, F.P., Murphy, J.M., Mesenchymal stem cells: clinical applications and biological characterization, *The International Journal of Biochemistry & Cell Biology* 36 (2004), 568-584
8. Bos, C., Delmas Y, Desmoulière A, Solanilla A, Hauger O, Grosset C, Dubus I, Ivanovic Z, Rosenbaum J, Charbord P, Combe C, Bulte JW, Moonen CT, Ripoche J, Grenier N, In vivo MR imaging of intravascularly injected magnetically labeled mesenchymal stem cells in rat kidney and

liver, *Radiology* 2004; 233(3):781-789

9. Bosnakovski, D., Mizuno M, Kim G, Takagi S, Okumura M, Fujinaga T, Chondrogenic Differentiation of Bovine Bone Marrow Mesenchymal Stem Cells (MSCs) in Different Hydrogels: Influence of Collagen Type II Extracellular Matrix on MSC Chondrogenesis, *Biotechnology and Bioengineering*, 2005
10. Brindle, K.M., Molecular imaging using magnetic resonance: new tools for the development of tumor therapy, *The British Journal of Radiology* 76 (2003), 111-117
11. Brittberg, M. et al., Treatment of deep cartilage defects in the knee with autologous chondrocyte transplantation, *N Engl J Med* 1994, 331: 889-895
12. Bulte, J.W., Duncan ID, Frank JA, In vivo magnetic resonance tracking of magnetically labeled cells after transplantation, *J Cereb Blood Flow Metab* 2002; 22: 899-907
13. Bulte, J.W., Kraitchman, D.L., Mackay, A.M., Pittenger, M.F., Chondrogenic differentiation of mesenchymal stem cells is inhibited after magnetic labeling with ferumoxides, *Blood* 2004; 104(10):3410-3412; author reply 3412-3413
14. Chen, C.W., Tsai YH, Deng WP, Shih SN, Fang CL, Burch JG, Chen WH, Lai WF, Type I and II collagen regulation of chondrogenic differentiation by mesenchymal progenitor cells, *J Orthop Res.* 2005 Mar, 23(2):446-53
15. Chin, J., *Radiol* 2004, 29:299-307
16. Csaki, C., Schneider PR, Shakibaei M, Mesenchymal stem cells as a potential pool for cartilage tissue engineering, *Ann Anat* 190 (2008), 395-412
17. Daldrup-Link, H.E., Rudelius M, Metz S, Piontek G, Pichler B, Settles M, Heinzmann U, Schlegel J, Oostendorp RA, Rummeny EJ, Cell tracking with gadophrin-2: a bifunctional contrast agent for MR imaging, optical imaging, and fluorescence microscopy, *European Journal of Nuclear Medicine and Molecular Imaging* Vol. 31, No. 9, September 2004
18. Daldrup-Link, H.E., Meier R, Rudelius M, Piontek G, Piert M, Metz S, Settles M, Uherek C, Wels W, Schlegel J, Rummeny EJ, In vivo tracking

- of genetically engineered, anti-HER2/neu directed natural killer cells to HER2/neu positive mammary tumors with magnetic resonance imaging, *European Radiology* (2005), 15:4-13
19. Daldrup-Link, H.E., Rudelius M, Oostendorp RA, Settles M, Piontek G, Metz S, Rosenbrock H, Keller U, Heinzmann U, Rummeny EJ, Schlegel J, Link TM, Targeting of hematopoietic progenitor cells with MR contrast agents, *Radiology* 2003; 228(3):760-767
 20. Dennis, J.E., Carbillet JP, Caplan AI, Charbord P, The STRO-1plus marrow cell population is multipotential, *Cells Tissues Organs* 2002, 170:73-82
 21. Digirolamo, C.M., Stokes D, Colter D, Phinney DG, Class R, Prockop DJ, Propagation and senescence of human marrow stromal cells in culture; a simple colony-forming assay identifies samples with the greatest potential to propagate and differentiate, *British Journal of Haematology* 1999, 107, 275-281
 22. El-Badri, N.S., Maheshwari A, Sanberg PR, Mesenchymal Stem Cells in Autoimmune Disease, *Stem Cells and Development* 13:463-472 (2004)
 23. Engström, M., Klasson A, Pedersen H, Vahlberg C, Käll PO, Uvdal K, High proton relaxivity for gadolinium oxide nanoparticles, *Magn Reson Mater Phy* (2006) DOI 10.1007/s10334-006-0039-x
 24. Fatouros, P.P., Corwin FD, Chen ZJ, Broaddus WC, Tatum JL, Kettenmann B, Ge Z, Gibson HW, Russ JL, Leonard AP, Duchamp JC, Dorn HC, In Vitro and in Vivo Imaging Studies of a New Endohedral Metallofullerene Nanoparticle, *Radiology* 2006, 240:756-764
 25. Fox, J.M., Chamberlain G, Ashton BA, Middleton J, Recent advances into the understanding of mesenchymal stem cell trafficking, *British Journal of Haematology* 2007, 137, 491-502
 26. Fox, M.B., Esveld DC, Valero A, Luttge R, Mastwijk HC, Bartels PV, van den Berg A, Boom RM, Electroporation of cells in microfluidic devices : a review, *Anal Bioanal Chem*, 2006, 385 : 474-485
 27. Frank J.A., Miller BR, Arbab AS, Zywicke HA, Jordan EK, Lewis BK, Bryant LH Jr, Bulte JW, Clinically Applicable Labeling of Mammalian and Stem Cells by Combining Superparamagnetic Iron Oxides and Transfection Agents, *Radiology* 2003, 228:480-487

28. Garcia-Castro, J., Trigueros C, Madrenas J, Pérez-Simón JA, Rodriguez R, Menendez P, Mesenchymal stem cells and their use as cell replacement therapy and disease modelling tool, *J. Cell. Mol. Med.* Vol. 12, No 6B, 2008, pp. 2552-2565
29. Gelse, K., von der Mark K, Aigner T, Park J, Schneider H, Articular cartilage repair by gene therapy using growth factor-producing mesenchymal stem cells, *Arthritis Rheum* 2003, 48:430-441
30. Geninatti Crich, S., Cabella C, Barge A, Belfiore S, Ghirelli C, Lattuada L, Lanzardo S, Mortillaro A, Tei L, Visigalli M, Forni G, Aime S, In Vitro and in Vivo Magnetic Resonance Detection of Tumor Cells by Targeting Glutamine Transporters with Gd-Based Probes, *J. Med. Chem.* 2006, 49, 4926-4936
31. Giannoni, P., Pagano A, Maggi E, Arbicò R, Randazzo N, Grandizio M, Cancedda R, Dozin B, Autologous chondrocyte implantation (ACI) for aged patients: development of the proper cell expansion conditions for possible therapeutic applications, *Osteo Arthritis and Cartilage* (2005) 13, 589-600
32. Greisberg, J.K., Wolf JM, Wyman J, Zou L, Terek RM, Gadolinium inhibits thymidine incorporation and induces apoptosis in chondrocytes, *Journal of Orthopaedic Research* 19 (2001), 797-801
33. Grimm, J., *Molecular Imaging – New Horizons for Radiology*, Medical Solutions 1/2003
34. Hengerer, A., Mertelmeier, T., *Molecular Biology for Medical Imaging*, *electromedica* 69 (2001) no.1
35. Henning, T.D., Saborowski O, Golovko D, Boddington S, Bauer JS, Fu Y, Meier R, Pietsch H, Sennino B, McDonald DM, Daldrup-Link HE, Cell labeling with the positive MR contrast agent Gadofluorine M, *Eur Radiol.* 2007 May, 17 (5): 1226-1234
36. Henning, T.D. et al., Long term MR signal characteristics of Ferucarbotran-labeled mesenchymal stem cells: Discrimination of intra- and extracellular iron oxides before and after cell lysis, In:14th Scientific Meeting of the International Society of Magnetic Resonance in Medicine. Seattle, 2006

37. Hornak, J.P., Chemical Contrast Agents, The Basics of MRI, 14th ed: 1996-2004
38. Hsiao, J.-K., Tai MF, Chu HH, Chen ST, Li H, Lai DM, Hsieh ST, Wang JL, Liu HM, Magnetic Nanoparticle Labeling of Mesenchymal Stem Cells Without Transfection Agent: Cellular Behavior and Capability of Detection With Clinical 1.5 T Magnetic Resonance at the Single Cell Level, *Magnetic Resonance in Medicine* 58:717-724, 2007
39. Im, G.I., Jung NH, Tae SK, Chondrogenic Differentiation of Mesenchymal Stem Cells Isolated from Patients in Late Adulthood: The Optimal Conditions of Growth Factors, *Tissue Engineering*, Volume 12, Number 3, 2006
40. Indrawattana, N., Chen G, Tadokoro M, Shann LH, Ohgushi H, Tateishi T, Tanaka J, Bunyaratvej A, Growth factor combination for chondrogenic induction from human mesenchymal stem cell, *Biochemical and Biophysical Research Communications* 320 (2004) 914-919
41. Ittrich, H., Lange C, Dahnke H, Zander AR, Adam G, Nolte-Ernsting C, Labeling of mesenchymal stem cells with different superparamagnetic particles of iron oxide and detectability with MRI at 3T, Aug 2005
42. Jaiswal, R.K. et al., Regulation of osteogenic and adipogenic differentiation of human adult mesenchymal stem cells through phosphorylation of MAP kinase, *J. Biol. Chem.* 275, 9645-9652
43. Johnstone, B., Hering TM, Caplan AI, Goldberg VM, Yoo JU, In Vitro Chondrogenesis of Bone Marrow-Derived Mesenchymal Progenitor Cells, *Experimental Cell Research* 238, 265-272, 1998
44. Jorgensen, C., Gordeladze J, Noel D, Tissue engineering through autologous mesenchymal stem cells, *Biotechnology* 2004, 15:406-410
45. Jung, C.W., Surface properties of superparamagnetic iron oxide MR contrast agents: ferumoxides, ferumoxtran, ferumoxsil, *Magn Reson Imaging* 1995; 13(5):675-691
46. Kiepe, D. et al., IGF-I-stimulated IGFBP-3 and -5 expression, April 21, 2005
47. Kingsley, D.M., The TGF- β Superfamily: New Members, New Receptors, and New Genetic Tests of Function in Different Organism, *Genes Dev*

1994, 8:133-146

48. Kostura, L., Kraitchman DL, Mackay AM, Pittenger MF, Bulte JW, Feridex labeling of mesenchymal stem cells inhibits chondrogenesis but not adipogenesis or osteogenesis, *NMR Biomedicine* 2004, 17:513-517
49. Kuroda, R., Usas A, Kubo S, Corsi K, Peng H, Rose T, Cummins J, Fu FH, Huard J, Cartilage Repair Using Bone Morphogenetic Protein 4 and Muscle-Derived Stem Cells, *Arthritis and Rheumatism* 2006, 54:433-442
50. Lee, J.W., Kim YH, Kim SH, Han SH, Hahn SB, Chondrogenic Differentiation of Mesenchymal Stem Cells and its Clinical Applications, *Yonsei Medical Journal*, Vol. 45, Suppl., pp. 41-47, 2004
51. Lewin, M., Carlesso N, Tung CH, Tang XW, Cory D, Scadden DT, Weissleder R, Tat peptide-derivatized magnetic nanoparticles allow in vivo tracking and recovery of progenitor cells, *Nat Biotechnol.* 2000, 18:410-414
52. Mailänder, V. et al., Methods and tools for labelling cellular therapeutics for MRI detection, *Cellular Therapy*, March 20, 2006
53. Mao, J.J., Stem-cell-driven regeneration of synovial joints, *Biol. Cell* 2005 97, 289-301
54. Marshak, D.R., Cambrex Corporation, Commercialization of Stem Cell Therapy
55. Metz, S., Bonaterra G, Rudelius M, Settles M, Rummeny EJ, Daldrup-Link HE, Capacity of human monocytes to phagocytose approved iron oxide MR contrast agents in vitro, *Eur Radiol* 2004, 14:1851-1858
56. Misselwitz, B., Platzek J, Radüchel B, Oellinger JJ, Weinmann HJ, Gadofluorine 8: initial experience with a new contrast medium for interstitial MR lymphography, *Magma* 1999 Aug, 8(3) :190-5
57. Mwale, F., Stachura D, Roughley P, Antoniou J, Limitations of Using Aggrecan and Type X Collagen as Markers of Chondrogenesis in Mesenchymal Stem Cell Differentiation, *Journal of Orthopaedic Research*, August 2006
58. Oude Engberink, R.D., van der Pol SM, Döpp EA, de Vries HE, Blezer EL, Comparison of SPIO and USPIO for in vitro labeling of human

- monocytes: MR detection and cell function, *Radiology* 2007, 243(2): 467-74
59. Pawelczyk, E., Arbab AS, Pandit S, Hu E, Frank JA, Expression of transferrin receptor and ferritin following ferumoxides-protamine sulfate labeling of cells : implications for cellular magnetic resonance imaging, *NMR Biomedicine* 2006, 19:581-592
 60. Prockop, D.J., Gregory CA, Spees JL, One strategy for cell and gene therapy : harnessing the power of adult stem cells to repair tissues, *Proc. Natl Acad. Sci. USA* 2003; 100:11917-11923
 61. Rafii, S., Mohle R, Shapiro F, Frey BM, Moore MA, Regulation of hematopoiesis by microvascular endothelium, *Leuk. Lymphoma* 27 (1997), 375-386
 62. Rapp, U.R., Ceteci F, Schreck R, Oncogene-induced plasticity and cancer stem cells, *Cell Cycle* 2008, 7(1): 45-51
 63. Raynal I., Prigent P, Peyramaure S, Najid A, Rebuzzi C, Corot C, Macrophage endocytosis of superparamagnetic iron oxide nanoparticles, *Invest Radiol.* 2004, 39, 56-63
 64. Reimer, P., Balzer, T., Ferucarbotran (Resovist): a new clinically approved RES-specific contrast agent for contrast-enhanced MRI of the liver: properties, clinical development, and applications, *Eur Radiol* 2003, 13:1266-1276
 65. Reiser M. SW., "Magnetresonanztomographie" Springer Verlag, Berlin, 1997, 15, 108-109
 66. Rousche, K.T., Knudson, C.B., *Matrix Biology* 21 (2002), 53-62
 67. Rummeny E.J., Reimer P., Heindel W., "Ganzkörper-MR-Tomographie" *Thieme*, Stuttgart, 2006, 24-30
 68. Saw, K.Y., Hussin P, Loke SC, Azam M, Chen HC, Tay YG, Low S, Wallin KL, Ragavanaidu K, Articular cartilage regeneration with autologous marrow aspirate and hyaluronic Acid: an experimental study in a goat model, *Arthroscopy*, 2009, Dec., 25 (12): 1, 391-400
 69. Simon, G.H., von Vopelius-Feldt J, Fu Y, Schlegel J, Pinotek G, Wendland MF, Chen MH, Daldrup-Link HE, Ultrasmall Superparamagnetic Iron

- Oxide-Enhanced Magnetic Resonance Imaging of Antigen-Induced Arthritis : A Comparative Study Between SHU 555 C, Ferumoxtran-10, and Ferumoxytol, *Investigative Radiology*, Volume 41(1), January 2006.45-51
70. Stoll, G., Wessig C, Gold R, Bendszus M, Assessment of lesion evolution in experimental autoimmune neuritis by gadofluorine M-enhanced MR neurography, *Experimental Neurology* 197 (2006), 150-156
 71. Sun, R., Dittrich J, Le-Huu M, Mueller MM, Bedke J, Kartenbeck J, Lehmann WD, Krueger R, Bock M, Huss R, Seliger C, Gröne HJ, Misselwitz B, Semmler W, Kiessling F, Physical and Biological Characterization of Superparamagnetic Iron Oxide- and Ultrasmall Superparamagnetic Iron Oxide-Labeled Cells, *Investigative Radiology*, Volume 40, Number 8, August 2005
 72. Toh, W.S., Liu H, Heng BC, Rufaihah AJ, Ye CP, Cao T, Combined effects of TGF β 1 and BMP2 in serum-free chondrogenic differentiation of mesenchymal stem cells induced hyaline-like cartilage formation, *Growth Factors*, Dec. 2005, 23(4): 313-321
 73. Tscheudschilsuren, G., Bosserhoff AK, Schlegel J, Vollmer D, Anton A, Alt V, Schnettler R, Brandt J, Proetzl G, Regulation of mesenchymal stem cell and chondrocyte differentiation by MIA, *Experimental Cell Research* 312 (2006), 63-72
 74. Tuan, R.S., Boland G, Tuli R, Adult mesenchymal stem cells and cell-based tissue engineering, *Arthritis Research and Therapy* 2003, 5:32-45
 75. Wagner, W., Ho AD, Zenke M, Different Facets of Aging in Human Mesenchymal Stem Cells, *Tissue Eng Part B Rev.* 2010 Mar. 2
 76. Wakitani, S., Goto T, Pineda SJ, Young RG, Mansour JM, Caplan AI, Goldberg VM, Mesenchymal cell-based repair of large, full-thickness defects of articular cartilage, *J Bone Joint Surg Am* 1994, 76:579-592
 77. Walczak, P., Kedziorek DA, Gilad AA, Lin S, Bulte JW, Instant MR Labeling of Stem Cells Using Magnetoelectroporation, *Magnetic Resonance in Medicine* 54:769-774 (2005)
 78. Wang, Y-X.J., Hussain SM, Krestin GP, Superparamagnetic iron oxide contrast agents : physicochemical characteristics and applications in MR imaging, *Eur. Radiol.* 2001, 11: 2319-2331

79. Weissleder, R., Mahmood, U., *Molecular Imaging, Radiology* 2001, 219:316-333
80. Will, O., Purkayastha S, Chan C, Athanasiou T, Darzi AW, Gedroyc W, Tekkis PP, Diagnostic precision of nanoparticle-enhanced MRI for lymph-node metastases: a meta-analysis, *Lancet Oncology* 2005, 7:52-60
81. Yang, I.H., Kim SH, Kim YH, Sun HJ, Kim SJ, Lee JW, Comparison of Phenotypic Characterization between “Alginate Bead” and “Pellet” Culture Systems as Chondrogenic Differentiation Models for Human Mesenchymal Stem Cells, *Yonsei Medical Journal*, Vol. 45, No. 5, pp. 891-900, 2004
82. Zipori, D., Mesenchymal stem cells: harnessing cell plasticity to tissue and organ repair, *Blood Cells, Molecules, and Diseases* 33 (2004) 211-215

8. Index of Tables and Figures

8.1 Tables

Table 1: Comparison of current therapies for synovial joint repair with stem-cell-based synovial joint condyle (Mao, 2005)

Table 2: Resovist versus Feridex/Endorem (Mailänder et al., 2006 ; Itrich et al., 2005 ; Wang et al., 2001 ; Arbab et al., 2004)

Table 3: Growth Factors (Johnstone et al., 1998; Mwale et al., 2006; Toh et al., 2005; Im et al., 2006; Indrawattana et al., 2004; Kiepe et al., 2005; Kingsley, 1994; Bosnakovski et al., 2006; Tscheudschilsuren et al., 2006)

Table 4: Detection of the Differentiation (Im et al., 2006; Toh et al., 2005; Indrawattana et al., 2004; Johnstone et al., 1998; Mwale et al., 2006; Rousche, Knudson, 2002; Tscheudschilsuren et al., 2006)

Table 5: Safranin O Staining

Table 6: Alcian Blue Staining

8.2 Figures

Figure 1: Chemical structure of Gadolinium-DTPA (Hornak, 1996-2004)

Figure 2: Differentiation Directions of Mesenchymal Stem Cells (Zipori, 2004)

Figure 3: Gene Expression Pattern of Mesenchymal Stem Cells (Zipori, 2004)

Figure 4: HMSCs plated in cell culture flasks

Figure 5: Chondrogenic pellets in culture tubes

Figure 6: 1.5 T Clinical MRI-Scanner

Figure 7: Histological Staining

Figures 8A-8I: Pellets

Figure 9: MR: Pellets on Day 14

Figure 10A: Labeling efficiency and viability (ferucarbotran)

Figure 10B: Labeling efficiency and viability (ferumoxides)

Figures 11A-11G: Histology

Figure 12A: Total GAG in media and pellets

Figure 12B: Total GAG dependent on days of prelabeling

9. Acknowledgement

I would like to thank Prof. Dr. Ernst J. Rummeny for the acceptance of my thesis at the Faculty of Radiology of the Technical University in Munich.

I would also like to thank Heike E. Daldrup-Link, MD, PhD, University of California in San Francisco, for the relinquishment of the topic and the supervision.

I thank Tobias D. Henning, MD, for the supervision and support of the experimental part of my thesis.

Furthermore, I thank Anne Kim for the GAG-quantification, Margaret Mayes for the histological stains, and Elizabeth J. Sutton, MD, for the MR images. Thanks to Andrew Horvai, MD, PhD, for the evaluation of the histological stains.

In the end, thanks to my parents for the moral and financial support that made this thesis possible.